The effects of collisional fragmentation on dust growth in protoplanetary disks

Department of Earth and Planetary Sciences,

Tokyo Institute of Technology

Ida laboratory

04M04119 Suyama, Toru

Abstract

Dust growth in protoplanetary disks is an important process in both planetesimals formation and the evolution of protoplanetary disk themselves. Collisions between dust grains can result in not only their coalescence but also fragmentation. The collisional fragmentation is able to prevent planetesimal formation. In this paper, we examine the effects of collsional fragmentation in the process of dust growth in laminar disks and turbulent disks. Fragmentation occurs at mutual collisions of grains, if the collisional velocity is larger than a certain critical velocity determined by the strength of grains. If we consider compact grains consisting of sub-micron monomers, the critical velocity is roughly estimated to be $\sim$3 m/s for H_2O ice grains and $\sim$0.3 m/s for silicate grains.

Next we examine the collisional velocity analytically and numerically. The collisional velocity increases as dust grains grow as long as they are coupled with the gas disk. If the collisional velocity attains to the above critical velocity, collisional fragmentation prevents further growth. We estimate such critical dust size for fragmentation for laminar disks and turbulent disks. In laminar disks, the collisional velocity depends on the height z. It is given by the vertical settling velocity above the midplane and by the radial velocity near the midplane. Since the collisional velocity is small at the midplane, compared with that at a high level, grains can grow larger at the midplane than above it. The collisional velocity at the midplane given by the radial velocity attains to the maximum value at a certain grain size. The maximum collisional velocity is given by 20-50 m/s, depending on the disk temperature. This maximum velocity is larger than the above critical velocity. Thus, collisional fragmentation limits dust growth at the whole disk.

We also consider the case of turbulent disk, assuming homogeneous and isotropic turbulence and adopting the so-called α-model. There are two effects of turbulence on the dust

growth and settling. One is the enhancement of the collisional velocity due to turbulent motion. The other one is the vertical diffusion of dust grains. These effects of disk turbulence prevent settling and growth of dust grains. As disk turbulence damps, dust grains would gradually settle and grow.

Since collisional fragmentation confines the dust size, it also confines the relative velocity of dust grains to the disk gas. As a result, the migration velocity of grains to the disk gas is limited to the critical velocity for fragmentation. There is some uncetainty in the critical velocity $V_{\rm frag}$. To fix it, further investigation on dust structure is needed.

Contents

1 Introduction

Planetary systems are formed in protoplanetary disks. Especially, the solid bodies like planets and asteroids are made from dust grains in protoplanetary disks. Dust grains grow through mutual collisions, gradually settle to the midplane of a disk and forms a dense dust layer at the midplane (e.g., Safronov 1969, Nakagawa et al. 1981). Then planetesimals would be formed in the dust layer through gravitational instability (Goldreich and Ward 1973) or simple coalescence (Weidenschilling and Cuzzi 1993). Then planets are formed from planetesimals through mutual collisions. Collisions between dust grains result in not only their coalescence but also fragmentation. If collisional fragmentation occur in a major part of collisions, it would prevent planetesimal formation. Therefore, it is important to estimate the effects of collsional fragmentation in the process of dust growth.

Recent observations with high resolution at various wavelengths gave us much information of dust grains in protoplanetary disks. Testi et al. (2003) observed a protoplanetary disk CQ Tauri with mm observations. They show dust grains grown to sizes as large as a few centimeters. van Boekel et al. (2003) observed some protoplanetary disks with mid-infrared spectroscopy. They show the evidence for the existence of small grains at surface layer in protoplanetary disks. Their typical samples are 10^6 yr old. Dullemond and Dominik (2005) examined dust coagulation in turbulent disks through the numerical calculation. According to their simulation of dust growth without fragmentation, the small grains are depleted on a time scale that is much shorter than time scale is consistent with the observations. They insist that collisional fragmentation is plausible mechanism to replenish small grains, assuming a small critical collisional velocity for fragmentation of 0.1 m/s.

Dust growth in protoplanetary disks have been investigated by many authors for both laminar disks (e.g., Safronov 1969; Weidenschilling 1980, 1997; Nakagawa et al. 1981, 1986) and turbulent disks (e.g., Weidenschilling 1984; Mizuno et al. 1988; Schmitt et al. 1997). For example, Nakagawa et al. (1981) examined the growth of dust grains in the cource of

dust settling solving the so-called coagulation equation. Weidenschilling (1984) examined the evolution of dust grains in turbulent disks through numerical calculation. In his calculation, the effects of collisional fragmentation is also included, through he assumed very strong turbulence with a typical of the sound speed. According to his result, the dust size distribution is in a steady state as a result of the equilibrium between grain growth and fragmentation. Although the effects of collisional fragmenation is also included in some other papers, they set the critical velocity for fragmentation to be one assumed value. Thus, it is not clear how the effect of collisional fragmentation on dust growth depends on the critical velocity.

Experimental and the theoretical studies on dust collisions done by many author recently. Thus, the quantitative investigation becomes possible. In protoplanetary disks, sub-micron interstellar particles grow to much larger dust grains through mutual collisions. The fragmentation occurs at mutual collisions of grains, if the internal pressure enhanced by the collision is larger than the tensile strength of the grains. This condition is satisfied for collisions with sufficiently high relative velocities. The critical velocity for fragmentation depends on the tensile strength. The tensile strength of dust grains is governed by an adhesion force between two sub-micron interstellar particles (or monomers) in contact. To describe the adhesion force between the monomers the model of Johnson, Kendall and Roberts (1971) (the so-called JKR model) is used in several papers (Chokshi et al. 1993, Dominik & Tielens 1995, Dominik & Tielens 1996, Dominik & Tielens 1997). Dominik and Tielens (1997) performed numerical simulations of aggregate collision, assuming the JKR model for interparticle forces and obtained the critical velocity for fragmentation. According to their results, the critical velocity is about 10 m/s for H_2O ice grains. On the other hand, Blum and Wurm (2000) performed collision experiments for SiO_2 grains in microgravity environment. They found that when collisional velocity is larger than 1.2 m/s, dust grains do not grow, which is consistent with the theoretical result by Dominik and Tilens (1997). We will further describe the criterion for collisional fragmentation in Chapter 2 in detail.

In this paper, we clarify the effects of collisional fragmentation on dust growth in laminar disks or turbulent disks. The outcomes of collisions are governed by collisional velocities as mentioned above. To examine the effects of collisional fragmentation, we evaluate the collisional velocity in the cource of the dust growth in laminar disks and discuss the dust growth including collsional fragmentation. We see that collisional fragmentation is effective in laminar disks only inner region ($r \lesssim 1$AU). However, after settling, collisional fragmentation occurs at midplane of the whole disk and the maximum dust size limited by fragmentation. We also examine tha case of turbulent disks.

In the gaseous disks, the gas drag force causes dust inward migration (e.g., Whipple 1972, Adachi et al. 1976). The dust radial migration changes the dust surface density, which governs the process of planetesimal formation. Thus, dust migration is important in the formation of planetesimals. Furthermore, some authors suggested that dust migration in anticyclonic eddies enhances that dust density and could even trigger a local gravitational instability (e.g., Barge and Sommeria 1995). In these migration process of dust grains, the migration velocity of dust grains increases with the dust size. Then collisional fragmentation can also confined the migration velocity of dust grains by regulating their size. We will discuss this effect of fragmentation on dust migration.

In the next section we describe the criterion for collisional fragmentation. In Section 3 and 4 we examine the collisional velocity of dust grains and clarify the effect of fragmentation on dust growth in laminar disks and turbulent disks. In Section 5 we summarised our results and also discuss the effect of fragmentation on the radial migration of dust grains and the motion of dust grains trapped in turbulent eddies.

2 The criterion for collisional fragmentation

2.1 Tensile strength of dust grains

In protoplanetary disks, sub-micron interstellar particles grow to much larger dust grains through mutual collisions. The fragmentation occurs at the mutual collisions of grains, if the internal pressure enhanced by the collision is larger than the tensile strength of the grains. This collisional fragmentation would prevent the dust growth. The strength of dust grains is governed by an adhesion force between two sub-micrion interstellar particles (or monomers) in contact. To describe the adhesion force between the monomers the model of Johnson, Kendall and Roberts (1971) (the so-called JKR model) is used in many papers (Chokshi et al. 1993, Dominik and Tielens 1995, Dominik and Tielens 1996, Dominik and Tielens 1997).

The JKR model is based on an earlier model by Hertz (1882). He examined deformation of two elastic solid spheres in contact under an external load but ignored interparticle attractive forces. The deformation results in an repulsive elastic force between the spheres, which is balanced with the external load. On the other hand, Johnson et al. (1971) took account of the attractive force due to the surface tension. In the JKR model, the net force between two particles in contact is given by the difference between the attractive force due to the surface tension and the repulsive elastic ones. The net force between two particles is dependent on the distance of the centers of them. It vanishes for an equilibrium distance that balances the attractive force with the repulsive elastic one. For a larger interparticle distance, the net force becomes attractive. Its magnitude increases with the displacement from the equilibrium distance an attains to a maximum value for a critical displacement. This maximum adhesion force between two spherical particles is given in JKR model by

$$F_{\rm sep} = \frac{3\pi}{2} a_0 \gamma \ , \tag{2.1}$$

where a_0 is the radius of the particle and γ is the surface energy of its unit area. For a external load larger than $F_{\rm sep}$, the bond between the particles is cut and the interparicle

force vanishes. The bond energy between two particles is roughly given by $\sim F_{\rm sep}\delta_c$, where δ_c is the critical displacement. Using this JKR model and assuming compact dust grains (or aggregates) consisted of sub-micron monomers, we can roughly estimate their tensile strength as (Sirono and Greenberg 2000)

$$Y \sim \frac{F_{\rm sep}}{\pi a_0^2} \sim \frac{3\gamma}{2a_0} \ . \tag{2.2}$$

We set $a_0 = 0.1\mu$m as a typical interstellar dust size. For H_2O grains, their tensile strength is estimated to be 2×10^6 Pa and for SiO_2 grains, it is 4×10^5 Pa. The material parameters we used employed are listed in Table 1. For very porous grains the tensile strength would be reduced much.

The JKR model has been checked experimentally. Heim et al. (1999) measured the adhesion force between two micron-sized spherical grains (SiO_2). Their result is consistent with JKR model. Blum and Scräpler (2004) measured the tensile strength of high-porosity dust aggregates with the filling factor of 0.2. Their samples are SiO_2 with monomer size $a_0 = 0.76$ μm and surface energy $\gamma = 0.014$ J/m^2. The obtained tensile strength is $\sim$1000 Pa and it is much smaller than the analytical estimated value $\sim$ 30000 Pa. This reduction in the tensile strength would be due to the high porosity of the aggregate.

2.2 The critical velocity for fragmentation

The internal pressure enhanced by a collision increases with the collisional velocity between the grains. If the collisional velocity is larger than a critical velocity and the internal pressure becomes larger than the tensile strength at the collision, the fragmentation occurs. To evaluate the critical velocity, we first estimate the internal pressure at a collision. The pressure at a collision $P_{\rm col}$ is approximately given by $\sim \rho_0 c_{\rm mat} V_{\rm col}$, where ρ_0 is the material density of the monomers, $c_{\rm mat}$ is the sound speed (in other words, the velocity with which the information propagates in dust grains) and $V_{\rm col}$ is the collisional velocity. The sound

speed $c_{\rm mat}$ is estimated as follows. The interparticle force between two particles in contact is approximately given by the restoring force with the spring constant $k \sim F_{\rm sep}/\delta_c$ where δ_c is the critical displacement in the JKR model. The critical displacement δ_c is given by $2.55[(1-\nu)^4\gamma^2 a_0/E^2]^{1/3}$, where ν and E are Poisson's ratio and Young's modulus of the monomer. After two grains collide with each other, the information propagates from contact point through the inside of the grains and each monomer stops in turn. The time required for each monomer to stop, Δt, is given by

$$\Delta t \sim \sqrt{\frac{m_0}{k}} \sim \sqrt{\frac{\rho_0 a_0 \delta_c}{Y}} \ , \tag{2.3}$$

where m_0 is the monomer mass. During the interval Δt, the information propagate by a distance of the monomer size. Then, the sound speed $c_{\rm mat}$ is given by

$$c_{\rm mat} \sim \frac{a_0}{\Delta t} \sim \sqrt{\frac{Y a_0}{\rho_0 \delta_c}} \ . \tag{2.4}$$

Using this expression $c_{\rm mat}$, we obtain the pressure enhanced at a collision $P_{\rm col}$ as

$$P_{\rm col} \sim V_{\rm col}\sqrt{\frac{\rho_0 a_0 Y}{\delta_c}} \ . \tag{2.5}$$

Finally, balancing the pressure $P_{\rm col}$ with the strength Y, we have for the critical velocity $V_{\rm frag}$:

$$V_{\rm frag} \sim \sqrt{\frac{Y}{\rho_0}\frac{\delta_c}{a_0}} \ . \tag{2.6}$$

The obtained critical velocity is independent of the dust size. The material parameters are listed in Table 1. If we set $a_0 = 0.1\mu$m (a typical interstellar dust size). The critical velocity is 3 m/s for H_2O grains and 0.3 m/s for SiO_2 grains. Chokshi et al. (1993) also estimated the critical velocity for collisional fragmentation in another way. They assumed that the collisional fragmentation occurs when the kinetic energy per a monomer, $(1/2)m_0 V_{\rm col}^2$, is larger than the bond energy between two monomers, $\sim F_{sep}\delta$. Their critical velocity in this way almost agrees with equation (2.6).

Table 1: Material parameters, tensile strengths and critical velocities.

material	γ (J/m^2)	E (Pa)	ν	ρ_{mat} (kg/m^3)	$\delta_c^{(a)}$ (Å)	Y (Pa)	$V_{\rm frag}$ (m/s)
H_2O	0.100	0.70×10^9	0.25	1000	5.98	2×10^6	3
SiO_2	0.025	0.54×10^{10}	0.17	2600	0.69	4×10^5	0.3

$^{(a)}\delta = 2.55[(1-\nu)^4\gamma^2 a_0/E^2]^{1/3}$ (Chokshi et al. 1993)

Dominik and Tielens (1997) performed numerical simulation of aggregate collision, assuming the JKR model for interparticle forces and also examined the critical velocity. According to their results, the critical velocity is $\sim$ 10 m/s for H_2O grains. They considered that when the collisional energy $\frac{1}{2}(1/m_1 + 1/m_2)V_{\rm col}^2$ equals the energy required to break all contact $n_c F_c \delta_c$, Loss of monomer starts (fragmention occurs). Here, m_1 and m_2 are the mass of aggregate, and n_c is the total number of contacts between monomers. Dominik and Tielens considered that the collisional energy is distributed over all contacts. On the other hand, Chokshi et al. considered that collisional fragmentation occurs when the collisional energy is larger than the energy required to break one contact. The critical velocity of Dominik and Tielens is about n_c times as large as one of Chokshi et al. Furthermore, Blum and Wurm (2000) performed the collision experiments for SiO_2 grains in microgravity environment. When collisional velocity is larger than 1.2 m/s, dust grains do not grow. These results of the previous studies are almost consistent with the our estimation.

In our theoretical estimation, it is assumed that dust grains are compact. However, dust grains may have porous structure in protoplanetary disks and the tensile strength of dust grains may be much smaller than our estimation. Then, at low-velocity collision, collisional fragmentation may also occur. In the numerical simulation by Dominik and Tielens (1997) and the experiments by Blum and Wurm (2000), they treat porous aggregates but only small ones. The tensile strength of much larger porous grains may be smaller than their results.

For example, tensile strength of high-prosity dust aggregates is ∼1000 Pa (Blum and Scräpler 2004) and it is much smaller than the analytical estimated value of 10^4 Pa. For such dust aggregates, the critical velocity is ~ 0.01 m/s.

3 Motion of dust grains and the collisional velocity in protoplanetary disks

In this chapter, we examine the collisional velocity at a collision between dust grains in protoplanetary disks. Dust grains we consider are wel coupled to disk gas. Thus, the collisional velocities are approximately given by the relative velocities of dust grains to gas. The relative velocities of dust grains and gas are determined by the balance between the gravitational force from the central star and the gas drag force. It is assumed that the velocities of dust grains and gas become the terminal velocities. We also consider the motion of dust grains in turbulent disks as well as that in laminar disks.

3.1 Disk model

We consider a passive protoplanetary disk around a solar-type central star with $1M_\odot$. To describe the disk, we use a cylindrical coordinate system (r, ϕ, z) of which the origin is located at the central star. The z-axis coincides with the rotation axis of the disk. We assume that the disk is isothermal in the vertical direction (i.e., in the z-direction).

Under this assumption, the vertical density distribution $\rho_g(z)$ of the gas component is given in the hydrostatic equilibrium by (Hayashi 1981)

$$\rho_g = \frac{\Sigma_g}{\sqrt{2\pi}H} \exp\left(-\frac{z^2}{2H^2}\right) , \tag{3.1}$$

where Σ_g is the surface density of disk gas and H is the gas scale height of the disk given by c_s/Ω_k. Furthermore, $\Omega_k = (GM_*/r^3)^{1/2}$ is the Keplerian angular velocity and $c_s =$

$(k_BT/\mu m_\mu)^{1/2}$ is the isothermal sound speed, where G, k_B, and m_μ are the gravitational constant, Boltzmann's constant, and the atomic mass unit, respectively, and T and μ are the disk temperature and the mean molecular weight, respectively. We set $\mu = 2.34$.

As for the surface density distribution of gaseous disks, according to Hayashi (1981) we adopt a power-law distribution of

$$\Sigma_g(r) = \Sigma_{g0} \left(\frac{r}{1\mathrm{AU}}\right)^{-\frac{3}{2}} \ , \tag{3.2}$$

where Σ_{g0} is the gas surface density at 1 AU. In the standard case of this study, we adopt the values of the minimum mass solar nebula (MMSN;Hayashi 1981), that is, $\Sigma_{g0} = 17000$ kg/m^2. We assume that dust grains is consisted of H_2O and organics. The dust-to-gas ratio ζ_d and the solid material density ρ_{mat} are set to be 0.014 and 1380 kg/m^3, respectively in the standard case. These values are consistent with the solar abundance when H_2O ice is included in grains (Pollack et al.1994).

In this study, we assume that the disk temperature profile is given by (Kusaka et al. 1970)

$$\sigma_{sb}T^4 = \frac{L_*}{8\pi r^2}\left[\frac{4}{3\pi}\frac{R_*}{r} + \frac{H}{r}\left(\frac{\partial \ln H}{\partial \ln r} - 1\right)\right] \ , \tag{3.3}$$

where, L_*, T_*, R_* are the luminosity, the surface temperature and the radius of the central star. At $H \ll R_*$(near the central star),

$$T = \left(\frac{2}{3\pi}\right)^{\frac{1}{4}} \left(\frac{R_*}{r}\right)^{\frac{3}{4}} T_* \ . \tag{3.4}$$

On the other hand, at $H \gg R_*$(far the central star),

$$T = \left(\frac{2T_*}{49T_c}\right)^{\frac{1}{7}} \left(\frac{R_*}{r}\right)^{\frac{3}{7}} T_* \ . \tag{3.5}$$

In the standard case we consider $L_* = 3.83 \times 10^{26}$ W, $T_* = 5780$ K and $R_* = 6.96 \times 10^8$ m, the temperature profile is given by

$$T = \begin{cases} 69.9 \left(\frac{r}{1\mathrm{AU}}\right)^{-\frac{3}{4}} \mathrm{K} & (H \ll R_*) \\ 99.4 \left(\frac{r}{1\mathrm{AU}}\right)^{-\frac{3}{7}} \mathrm{K} & (H \gg R_*) \ . \end{cases} \tag{3.6}$$

3.2 Gas drag force

When dust grains move against the disk gas, they receive the gas drag force. The gas drag force governs the dust motion. Adachi et al. (1976) examined the gas drag effects on solid bodies in protoplanetary disks. For a spherical grain that is embedded in gas, the gas drag force is given by

$$\mathbf{F}_D = \frac{1}{2} C_D \pi a^2 \rho_g |\mathbf{V_{rel}}| \mathbf{V_{rel}} \tag{3.7}$$

$$= -mA\rho_g \mathbf{V_{rel}} \tag{3.8}$$

with

$$A = \frac{3|\mathbf{V_{rel}}|}{8\rho_{mat} a} C_D \ , \tag{3.9}$$

where C_D is the non-dimensional drag coefficient and $\mathbf{V_{rel}}$ is the relative velocity of the dust grain to the disk gas. Here, a and m are the radius and the mass of the grain, respectively. The drag coefficient C_D is given by

$$C_D \simeq \left[\left(\frac{24}{\mathcal{R}} + \frac{40}{10 + \mathcal{R}} \right)^{-1} + \frac{3\mathcal{M}}{8} \right]^{-1} + \frac{(2-\omega)\mathcal{M}}{1+\mathcal{M}} + \omega, \tag{3.10}$$

where $\mathcal{M}$ is the Mach number, $\mathcal{R}$ is the Reynolds number and ω is the correctional term. Here, the Mach number $\mathcal{M}$ and the Reynolds number $\mathcal{R}$ are defined by

$$\mathcal{M} = \frac{|\mathbf{V_{rel}}|}{c_t} \tag{3.11}$$

and

$$\mathcal{R} = \frac{6a|\mathbf{V_{rel}}|}{l_g c_t}, \tag{3.12}$$

respectively, where l_g is the mean free path of gas molecules, c_t is the thermal velocity. The mean free path is given by $l_g = \mu m_\mu / (\rho_g \sigma_{mol})$ and the thermal velocity is given by $c_t = \sqrt{\pi/8} c_s$. The correctional term ω is $\simeq 0.4$ at $\mathcal{R} \leq 2 \times 10^5$, and $\simeq 0.2$ at $\mathcal{R} \geq 2 \times 10^5$.

For $\mathcal{R} \ll 1$ and $\mathcal{M} \ll 1$, this case is divided further into two cases, depeneding on the values of the Knudsen number $\mathcal{K}(= a/l_g = \mathcal{R}/6\mathcal{M})$. For $\mathcal{K} \geq \frac{2}{3}$ $(a \leq \frac{3}{2} l_g)$, C_D and A are given by

$$C_D = \frac{8}{3\mathcal{M}} \quad A = \frac{c_t}{\rho_{mat} a} \ , \tag{3.13}$$

respectively. This case corresponds to Epstein's law. On the other hand, for $\mathcal{K} < \frac{2}{3}$ $(a > \frac{3}{2} l_g)$, C_D and A are given by

$$C_D = \frac{24}{\mathcal{R}} \quad A = \frac{3 l_g c_t}{2 \rho_{mat} a^2} \ , \tag{3.14}$$

respectively. This case corresponds to Stokes' law. In these two cases, A is independent on $\mathrm{v_{rel}}$. Therefore, as an expression of the gas drag force, the equation (3.8) is more useful than equation (3.7). In the case of a large Reynolds number $\mathcal{R} > 100$, on the other hand, C_D is given by

$$C_D = \begin{cases} 0.5 & (\mathcal{M} < 1) \\ 2 & (\mathcal{M} > 1) \end{cases} \tag{3.15}$$

In this case, therefore, the equation (3.7) is more useful.

3.3 The motion of dust grains in laminar disks

Nakagawa et al. (1986) derived the equation of motion of dust grains and gas in laminar disks, assuming the terminal velocities of dust grains. They considered equal-sized grain. Tanaka et al. (2005) derived the equation of motion of dust grains and gas when grains have a size distribution. We derived, along the line of Tanaka et al. (2005), the velocities of dust grains and gas. When grains have a size distribution, the equations of motion for gas and dust grains are given by

$$\frac{\partial \mathbf{U}}{\partial t} + [\mathbf{U} \cdot \nabla]\mathbf{U} = -A\rho_g[\mathbf{U} - \mathbf{u}] - \frac{GM_*}{|x|^3}\mathbf{x} \tag{3.16}$$

$$\frac{\partial \mathbf{u}}{\partial t} + [\mathbf{u} \cdot \nabla]\mathbf{u} = -\int Amn(m)[\mathbf{u} - \mathbf{U}]dm - \frac{GM_*}{|x|^3}\mathbf{x} - \frac{1}{\rho_g}\nabla P_g \ , \tag{3.17}$$

where $\mathbf{U}$ is the dust velocity and $\mathbf{u}$ is the gas velocity. The gas pressure P_g is given by $c_s^2\rho_g$. In equation (3.17), $n(m)dm$ denotes the number density of grains with masses between m and $m+dm$ at a height z. Thus, $n(m)$ describes the distribution of grains with respect to m (or the size a). We introduce a differentially rotating coordinate system with the Keplerian velocity. Instead of $\mathbf{U}$ and $\mathbf{u}$, we use the velocities $\mathbf{V} \equiv \mathbf{U} - r\Omega\mathbf{e}_\phi$ and $\mathbf{v} \equiv \mathbf{u} - r\Omega\mathbf{e}_\phi$ in the rotational frame. In the rotational frame, the equation on motion is rewritten by

$$\frac{\partial V_r}{\partial t} + V_r\frac{\partial V_r}{\partial r} + \frac{V_\phi}{r}\frac{\partial V_r}{\partial \phi} + V_z\frac{\partial V_r}{\partial z} - \frac{V_\phi^2}{r} = -A\rho_g(V_r - v_r) + 2\Omega_k V_\phi \tag{3.18}$$

$$\frac{\partial V_\phi}{\partial t} + V_r\frac{\partial V_\phi}{\partial r} + \frac{V_\phi}{r}\frac{\partial V_\phi}{\partial \phi} + V_z\frac{\partial V_\phi}{\partial z} - \frac{V_r V_\phi}{r} = -A\rho_g(V_\phi - v_\phi) - \frac{1}{2}\Omega_k V_r \tag{3.19}$$

$$\frac{\partial V_z}{\partial t} + V_r\frac{\partial V_z}{\partial r} + \frac{V_\phi}{r}\frac{\partial V_z}{\partial \phi} + V_z\frac{\partial V_z}{\partial z} = -A\rho_g(V_z - v_z) + \Omega_k^2 z \ , \tag{3.20}$$

and

$$\frac{\partial v_r}{\partial t} + V_r\frac{\partial v_r}{\partial r} + \frac{V_\phi}{r}\frac{\partial v_r}{\partial \phi} + V_z\frac{\partial v_r}{\partial z} - \frac{v_\phi^2}{r} = -\int Amn(m)(v_r - V_r)dm + 2\Omega_k v_\phi - \frac{1}{\rho_g}\frac{\partial P}{\partial r} \tag{3.21}$$

$$\frac{\partial v_\phi}{\partial t} + V_r\frac{\partial v_\phi}{\partial r} + \frac{V_\phi}{r}\frac{\partial v_\phi}{\partial \phi} + V_z\frac{\partial v_\phi}{\partial z} - \frac{v_r v_\phi}{r} = -\int Amn(m)(v_\phi - V_\phi)dm - \frac{1}{2}\Omega_k v_r - \frac{1}{\rho_g r}\frac{\partial P}{\partial \phi} \tag{3.22}$$

$$\frac{\partial v_z}{\partial t} + V_r\frac{\partial v_z}{\partial r} + \frac{V_\phi}{r}\frac{\partial v_z}{\partial \phi} + V_z\frac{\partial v_z}{\partial z} = -\int Amn(m)(v_z - V_z)dm + \Omega_k^2 z - \frac{1}{\rho_g}\frac{\partial P}{\partial z} \ . \tag{3.23}$$

Since $\mathbf{V}$ and $\mathbf{v}$ are much smaller than the Keplerian velocity, we can neglect the second-order terms of these velocities in the equations of the motion. Then, setting $\dfrac{\partial}{\partial t} = 0$ (steady state) and $\dfrac{\partial}{\partial \phi} = 0$ (axial symmetry), we obtain the velocities of gas and grains in the rotating cylindrical coordinates. The velocities of dust grains are given by

$$V_r = \frac{\Gamma^2 v_r + 2\Gamma v_\phi}{1+\Gamma^2} \tag{3.24}$$

$$V_\phi = \frac{-\Gamma v_r + 2\Gamma^2 v_\phi}{2(1+\Gamma^2)} \tag{3.25}$$

$$V_z = v_z - \frac{1}{\Gamma}\frac{z}{r}v_k \ , \tag{3.26}$$

and the velocity of gas is given by

$$v_r = \frac{2\lambda_1}{(1+\lambda_2)^2+\lambda_1^2}\eta v_k \tag{3.27}$$

$$v_\phi = -\frac{(1+\lambda_2)}{(1+\lambda_2)^2+\lambda_1^2}\eta v_k \tag{3.28}$$

where

$$\Gamma = \frac{\rho_g A}{\Omega_k} \tag{3.29}$$

$$\lambda_k = \int \frac{\Gamma^k}{1+\Gamma^2}\frac{mn(m)}{\rho_g}dm \tag{3.30}$$

$$\eta = -\frac{1}{2r\Omega_k^2\rho_g}\frac{\partial P}{\partial r} \ . \tag{3.31}$$

Thus, the relative velocity between dust grains and gas is given by

$$V_r - v_r = \frac{-v_r + 2\Gamma v_\phi}{1+\Gamma^2} \tag{3.32}$$

$$V_\phi - v_\phi = \frac{-\Gamma v_r - 2v_\phi}{2(1+\Gamma^2)} \tag{3.33}$$

$$V_z - v_z = -\frac{1}{\Gamma}\frac{z}{r}v_k \ . \tag{3.34}$$

When the dust density is much smaller than the density of gas $mn(m)/\rho_g \ll 1$, λ_k is ~ 0. Then, the relative velocity between dust grains and gas is given by

$$V_r - v_r = -\frac{2\Gamma}{1+\Gamma^2}\eta v_k \tag{3.35}$$

$$V_\phi - v_\phi = \frac{1}{1+\Gamma^2}\eta v_k \tag{3.36}$$

$$V_z - v_z = -\frac{1}{\Gamma}\frac{z}{r}v_k \ . \tag{3.37}$$

The relative velocity is governed by Γ, η. We use equations (3.35), (3.36) and (3.37) as the relative velocity between dust grains and gas.

The non-dimensional parameter $1/\Gamma$ means that the frictional time for gas drag normalized by the Keplerian period. For small grains, Γ is large and the velocity of such grains nearly equal the velocity of gas. The non-dimensional parameter Γ with similar uses as A

and C_D. For Epstein's law, Γ is given by

$$\Gamma = \frac{\rho_g A}{\Omega_k} = \frac{c_t}{\Omega_k a}\frac{\rho_g}{\rho_{mat}} = \frac{2}{\pi}\frac{\Sigma_g}{\rho_{mat} a}\exp\left(-\frac{z^2}{2H^2}\right) \ . \tag{3.38}$$

And for Stokes' law, Γ is given by

$$\Gamma = \frac{\rho_g A}{\Omega_k} = \frac{3}{2}\frac{l_g c_t}{\Omega_k a^2}\frac{\rho_g}{\rho_{mat}} = \sqrt{\frac{18}{\pi}}\frac{\mu m_\mu}{\rho_{mat}\sigma_{col}}\frac{H}{a^2} \ . \tag{3.39}$$

In these cases, Γ is independent of the velocity. In the case where $\mathcal{R} > 100$, Γ is given by

$$\Gamma = \frac{3}{8}\frac{\rho_g}{\Omega_k}\frac{\mathbf{V_{rel}}}{\rho_{mat} a}C_D \ . \tag{3.40}$$

Therefore, Γ depends on the velocity. For $V \simeq V_z$ ($V_z \gg V_r, V_\phi$), the equations of motion of dust grains are given by

$$V_r\frac{\partial V_z}{\partial r} + V_z\frac{\partial V_z}{\partial z} = -\frac{3C_D}{8}\frac{\rho_g}{\rho_{\rm mat} a}(V_z - v_z)^2 + \Omega_k^2 z \ . \tag{3.41}$$

At high altitude, that assuming ($V \simeq V_z$) is valid. We compare the each terms in equation (3.41). Since V_r, V_ϕ, V_z are much smaller than the Keplerian velocity, the dominant term is the second term of the right hand side $\Omega_k^2 z$. We compare the second-order terms. In the left hand side, the first term is $\sim V_r V_z/r$ and the second term is $\sim V_z^2/H$. The ratio of the first term to the second term is

$$\frac{V_r\frac{\partial V_z}{\partial r}}{V_z\frac{\partial V_z}{\partial z}} \sim \frac{V_r}{V_z}\frac{H}{r} = 2\times 10^{-2}\frac{V_r}{V_z}\left(\frac{r}{1\rm AU}\right)^{\frac{2}{7}} \ . \tag{3.42}$$

Here, we assume $V_{\rm rel} \simeq V_z$ ($V_z \gg V_r, V_\phi$). Thus, V_r/V_z is much smaller than unity. Therefore, the second term is much larger than the first term. At $z \lesssim H$ the first term of the right hand side (gas drag force) is $\sim 1/(\rho_{\rm mat} a)(\Sigma_g/H)V_z^2$. The ratio of the second term of the left hand side to the first term of the right hand side is given by

$$\frac{V_z\frac{\partial V_z}{\partial z}}{\frac{3C_D}{8}\frac{\rho_g}{\rho_{\rm mat} a}(V_z - v_z)^2} \sim \frac{\rho_{\rm mat} a}{\Sigma_g} \sim 0.1\left(\frac{a}{1\rm m}\right)\left(\frac{r}{1\rm AU}\right)^{\frac{3}{2}} \ . \tag{3.43}$$

Thus, $a \lesssim 1$ m at $r \lesssim 1$ AU the first term of the right hand side is much larger than the second term of the left hand side. Then, the equation (3.41) is written as

$$\frac{3C_D}{8}\frac{\rho_g}{\rho_{\rm mat} a}(V_z - v_z)^2 = \Omega_k^2 z \ . \tag{3.44}$$

Equation of motion is written as (3.44) for large grains at inner disk. Because at inner disk, for large grains the Reynolds number is large, our approximation equation (3.44) is valid. Thus, when the Reynolds number is large, the relative velocity $V_z - v_z$ is given by

$$V_z - v_z = -(2\pi)^{\frac{1}{4}} \sqrt{\frac{8}{3C_D} \frac{\rho_{\rm mat} a}{\Sigma_g} \frac{z}{H}} \exp\left(\frac{z^2}{4H^2}\right) c_s \ . \tag{3.45}$$

The parameter ηV_k means the difference between the gas velocity and the Kepler velocity due to the pressure gradient force. From equation (3.4) and (3.2) η is given by

$$\eta = (p + 3 + 2q) \left(\frac{c_{s0}}{v_{k0}}\right)^2 r_{\rm AU}^{1-p}, \tag{3.46}$$

respectively, where p and q are the power law index of radial distribution of temperature and gas density. Here, c_{s0}, v_{k0} are sound speed and Kepler velocity at 1 AU. η only depends on the distance from the central star. In the standard case, ηv_k is given by

$$\eta v_k = \begin{cases} 20.3 \left(\frac{r}{1\rm AU}\right)^{-\frac{1}{4}} \ {\rm m/s} & (H \ll R_*) \\ 19.3 \left(\frac{r}{1\rm AU}\right)^{\frac{1}{14}} \ {\rm m/s} & (H \gg R_*) \ . \end{cases} \tag{3.47}$$

On the other hand, in Hayashi model the temperture profile is given by $T = 280(r/1{\rm AU})^{1/2}$ K (Hayashi et al. 1981). In such a case, ηv_k is given by 50 m/s. The velocity of Hayashi model is about three times greater than the velocity of Kusaka model (standard case).

We show the velocities of dust grains in Figure 1. At high altitude, the z-component (the solid line) of the relative velocity between dust grains and gas is much larger than other components. While at midplane the r-component (the dashed line) of the relative velocity is much larger than other components. Thus, the relative velocity is written as follows:

At high altitude

$$\mathbf{V_{rel}} \simeq (V_z - v_z)\mathbf{e_z} = -\frac{1}{\Gamma}\frac{z}{r} v_k \mathbf{e_z} \tag{3.48}$$

At midplane, for $\Gamma \geq 1$

$$\mathbf{V_{rel}} \simeq (V_r - v_r)\mathbf{e_r} = -\frac{2}{\Gamma} \eta v_k \mathbf{e_r} \tag{3.49}$$

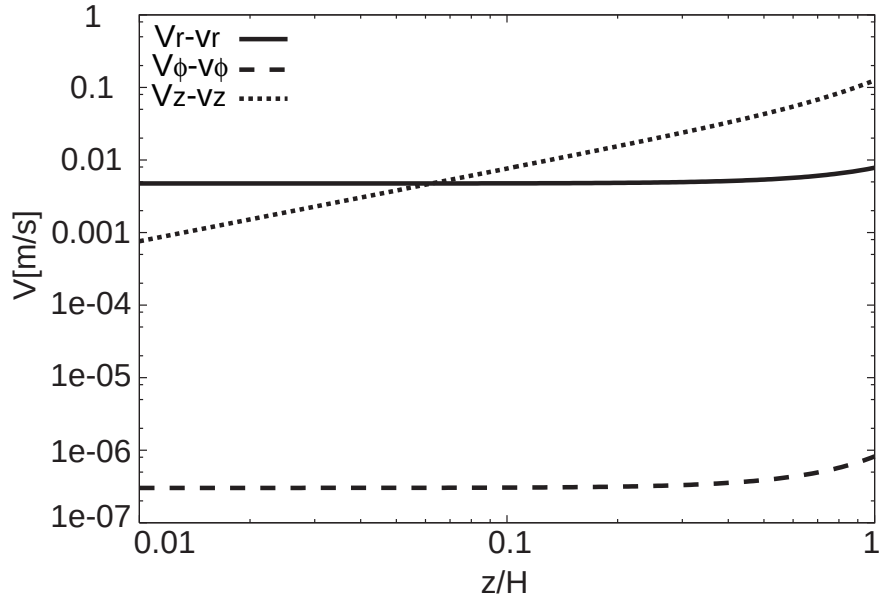

Figure 1: The height dependence of the relative velocity between dust and gas at $r = 1\mathrm{AU}, a = 1\mathrm{mm}$. The solid line, the dashed line and the dotted line are $V_r - v_r, V_\phi - v_\phi, V_z - v_z$, respectively.

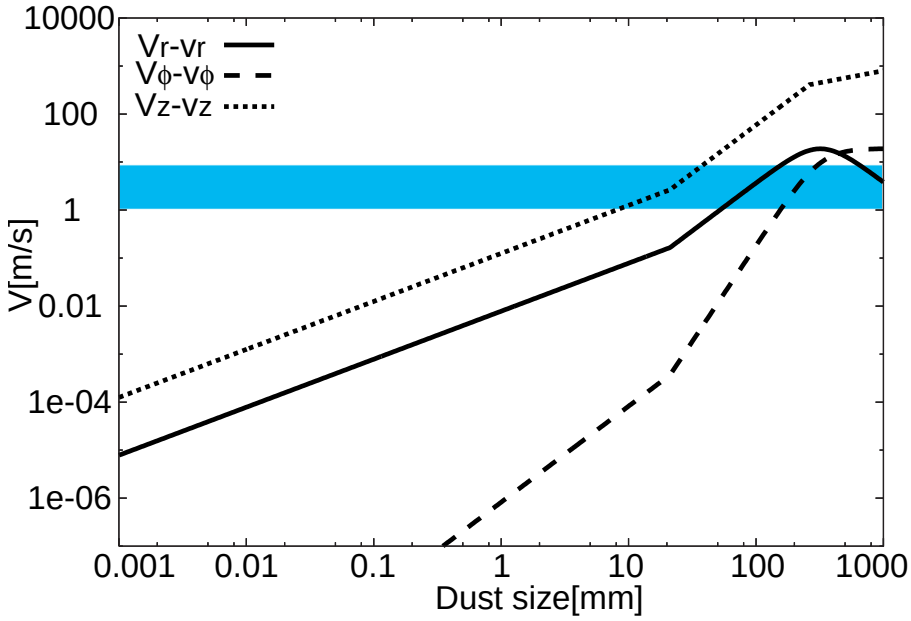

Figure 2: The size dependence of the relative velocity between dust and gas at $r = 1\mathrm{AU}, z = H$. The solid, the dashed and the dotted lines are $V_r - v_r, V_\phi - v_\phi$ and $V_z - v_z$, respectively. The hatched region shows the critical velocity V_{frag}.

At midplane, for $\Gamma \leq 1$

$$\mathbf{V_{rel}} \simeq (V_\phi - v_\phi)\mathbf{e}_\phi = -\eta v_k \mathbf{e}_\phi \tag{3.50}$$

The height where $V_z - v_z = V_r - v_r$ is given by

$$z = \frac{2\Gamma^2}{1+\Gamma^2}\eta r \ . \tag{3.51}$$

At $z \leq [2\Gamma^2/(1+\Gamma^2)]\eta r$, the velocities of dust grains is given by $V = V_r$. The radial velocity $V_r - v_r$ is almost independent of the height z at $z \lesssim H$. Thus, the velocity $V_{\rm rel}$ is almost independent of the height z at $z \lesssim H$.

The collisional velocities are roughly given by the relative velocities between dust grains and gas. In collision between small dust grain and large dust grain, the collisional velocity is determined by the velocity of the larger dust grain. On the other hand, the collisional velocities vanish in collisions between equal-sized dust grains. However, such collisions hardly occur. Thus, collisional velocities are the velocities of dust grains. We use the equation (3.35), (3.36), (3.37) and (3.45) as the collisional velocity in laminar disk.

Figure 2 shows collisional velocities at $r = 1$ AU, $z = H$. As the dust size becomes larger, the collisional velocity becomes large. Thus, as dust grains grow, dust grains have the larger velocity. When collisional velocity is larger than the critical velocity $V_{\rm frag}$, collisional fragmentation occurs. The critical velocity is 1-10 m/s because dust grains are composed of H_2O ice at $r = 1$ AU (the belt in Figure 2). The dust grains with $a \gtrsim 1 - 10$ mm has the collisional velocity $(V_z - v_z)$ that is larger than the critical velocity. For such dust grains collisional fragmentation occurs and the growth of dust grains are prevented. Thus, the maximum dust size is $\sim 1 - 10$ mm at $r = 1$ AU, $z = H$. The maximum dust size $a_{\rm frag}$ is defined by $V_z - v_z = V_{\rm frag}$. For Epstein's law the maximum dust size $a_{\rm frag}$ is given by

$$a_{\rm frag} = \frac{2}{\pi}\frac{\Sigma_g}{\rho_{\rm mat}}\frac{V_{\rm frag}}{c_s}\frac{H}{z}\exp\left(-\frac{z^2}{2H^2}\right) \ . \tag{3.52}$$

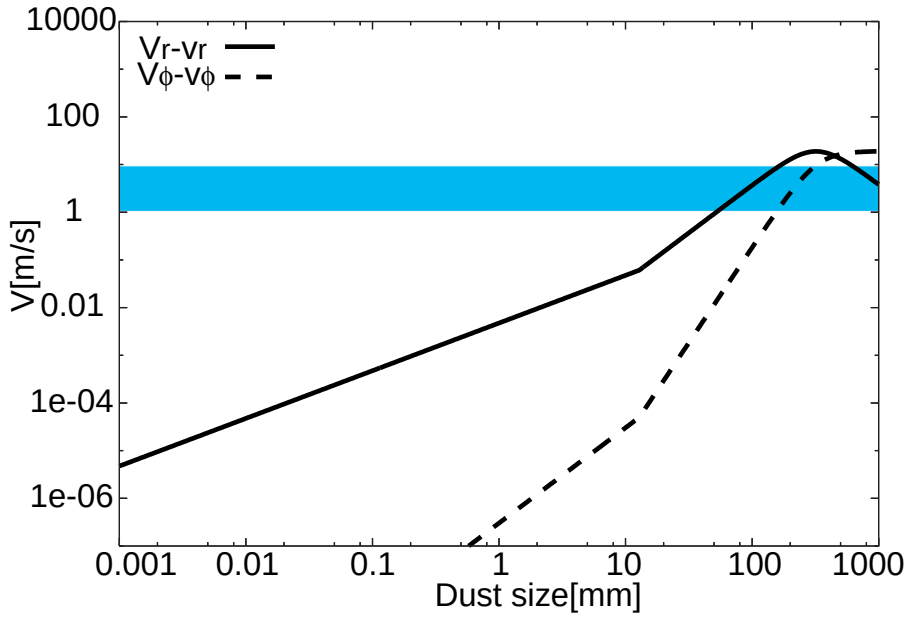

Figure 3: The size dependence of the relative velocity between dust and gas at $r = 1\mathrm{AU}, z = 0$ (midplane). The solid line and the dashed line are $V_r - v_r, V_\phi - v_\phi$, respectively. At $z = 0$ the vertical collisional velocity is vanished ($V_z = 0$). The hatched region shows the critical velocity V_{frag}.

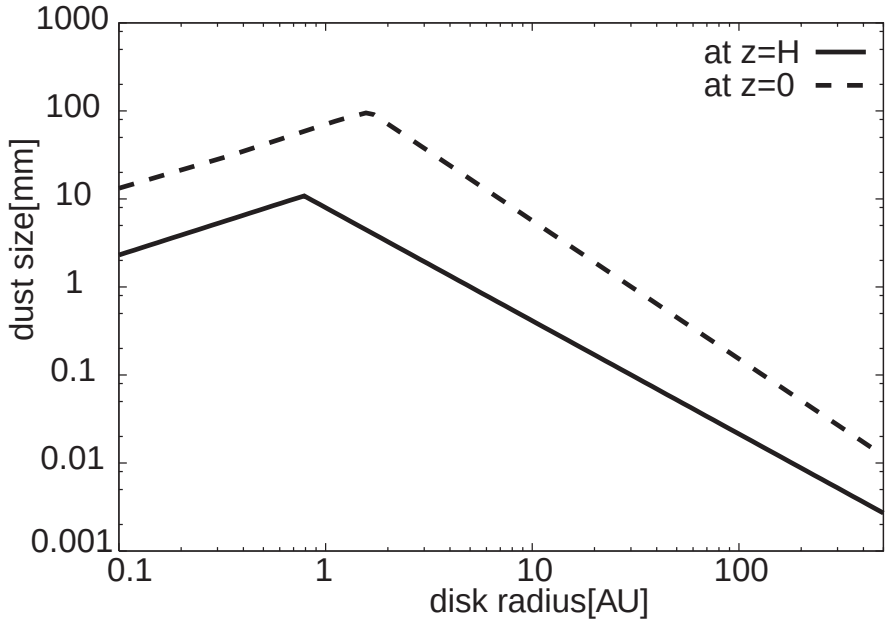

Figure 4: The maximum dust size a_{frag} for $V_{\mathrm{frag}} = 1$ m/s at r= 1AU. The solid line and the dashed line are at $z = H$ and $z = 0$, respectively.

For Stokes' law the maximum dust size $a_{\rm frag}$ is given by

$$a_{\rm frag} = \left(\frac{18}{\pi}\right)^{\frac{1}{4}} \sqrt{\frac{\mu m_\mu}{\rho_{\rm mat}\sigma_{\rm col}} \frac{V_{\rm frag}}{\Omega_k} \frac{H}{z}} \ . \tag{3.53}$$

The maximum dust size is determined by $a_{\rm frag}$ (equation (3.52) and (3.53)) at high altitude. However, large dust grains have the large settling velocity. Such large dust grains settle before they further grow. Therefore, the maximum dust size is determined by fragmentation and sedimentation.

Figure 3 shows collisional velocities at $r = 1$ AU, $z = 0$ (midplane). At midplane, the radial component of collisional velocity is much larger than the other components. Thus, The maximum dust size $a_{\rm frag}$ is defined by $V_r - v_r = V_{\rm frag}$. For Epstein's law $a_{\rm frag}$ is given by

$$a_{\rm frag} = \frac{2\sqrt{2}}{\pi e} \frac{V_{\rm frag}}{\eta v_k} \frac{\Sigma_g}{\rho_{\rm mat}} \ . \tag{3.54}$$

For Stokes' law $a_{\rm frag}$ is given by

$$a_{\rm frag} = \left(\frac{18}{\pi}\right)^{\frac{1}{4}} \sqrt{\frac{\mu m_\mu}{\rho_{\rm mat}\sigma_{\rm col}} \frac{V_{\rm frag}}{\eta v_k} H} \ . \tag{3.55}$$

At midplane the maximum dust size is determined by fragmentation only. We show $a_{\rm frag}$ in figure 4. At $r \gtrsim 1$ AU, gas drag law corresponds to Epstein's law. Then, as r decreases (dust grains migrate inward), $a_{\rm frag}$ increases. However, at $r \lesssim 1$ AU, gas drag law corresponds to Stokes' law. Then, $a_{\rm frag}$ decreases with r. At $r \simeq 1$ AU, $a_{\rm frag}$ becomes the maximum value.

3.4 Dust motion in turbulent disks

Protoplanetary disks are thought to be turbulent, which needed for their vicous evolution within typical disk lifetime of $\sim 10^{6-7}$ years. Turbulent gas motions would induce random velocities of small dust grains that are embedded in the gas and also enhance their collisional velocity. Within large eddies the friction forces from the gas lead to strongly correlated velocities for neighboring grains, whereas small eddies cause uncorrelated grain motions. In this section, we explain the model of turbulence in protoplanetery disks and estimate the collisional velocity in turbulent disks.

3.4.1 Homogeneous isotropic turbulence

We assume that turbulent motion is homogeneous and isotoropic in portoplanetary disks. Turbulent motion consists of various size of eddies.

The kinetic energy is transferred from the largest eddies to the smallest ones, the viscosity of the disk gas becomes important only for the smallest eddies and the kinetic energy is dissipated. Practically no energy dissipation occurs in larger eddies. To maintain the turbulento motion, external energy sources continually supply energy to the large eddies.

In the small scale l ($l \ll L$), the eddies have a similarity law. The energy supply occurs only for the largest eddies. The parameters that determine the nature of the eddies are the energy supply per unit mass per unit time of fluid ϵ and the molecular viscosity ν in homogeneous and isotropic turbulence. The energy supply occurs only for the largest eddies. Dimensional arguments (Tennekes and Lumley 1972) imply that the energy supply per unit mass is of order

$$\epsilon \sim \frac{v_L^3}{L}, \tag{3.56}$$

where L and v_L are the size and the velocity of the largest eddy. For eddies with a intermediate scale, the effects of viscous is not important and thus, the velocity and the period of such eddies expressed with the eddy size l and the energy deposition rate ϵ. The velocity and the period of eddies are given by

$$v_l \sim (\epsilon l)^{\frac{1}{3}} \tag{3.57}$$

$$t_l \sim \left(\frac{\epsilon}{l^2}\right)^{\frac{1}{3}} \ . \tag{3.58}$$

To express v_l as the function of t_l, we eliminate l from the equation (3.57) and (3.58). Then, the velocity of eddies is given by

$$v_l \sim (\epsilon t_l)^{\frac{1}{2}} \ . \tag{3.59}$$

Equation (3.59) is the usefull expression. The smallest eddies have the velocity, the length

and the period given by

$$v_i \sim (\nu_{\rm mol}\epsilon)^{\frac{1}{4}} \tag{3.60}$$

$$l_i \sim \left(\frac{\nu_{\rm mol}^3}{\epsilon}\right)^{\frac{1}{4}} \tag{3.61}$$

$$t_i \sim \left(\frac{\nu_{\rm mol}}{\epsilon}\right)^{\frac{1}{2}}, \tag{3.62}$$

where $\nu_{\rm mol}$ is the molecular viscousity.

3.4.2 α model

The diffusion an the angular momentum transfer due to the turbulent motion are described by the turbulent viscosity $\nu_{\rm turb}$. The turbulent viscosity $\nu_{\rm turb}$ is given in the so-called α model by (Shakura and Sunyaev 1973)

$$\nu_{\rm turb} = \alpha c_s H \ , \tag{3.63}$$

α is non-dimensional small parameter determines the strength of turbulence.

The most probable origin of disk turbulence is magneto-hydrodynamic (MHD) instability. The strengest turbulence due to MHD instability makes $\alpha \simeq 10^{-2}$. In order to obtain the expresion of the energy supply rate ϵ to turbulence, we assume that the size L and the velocity v_L of the largest eddies are

$$v_L \sim \alpha^{\frac{1}{2}} c_s, \qquad L \sim \alpha^{\frac{1}{2}} \frac{c_s}{\Omega_k} \tag{3.64}$$

respectively, as done in the previous studies (Schräpler and Henning 2004, Dullemond and Dominik 2004). Substituting (3.64) into (3.56), the energy deposition rate ϵ given by

$$\epsilon \sim \alpha c_s^2 \Omega_k \ . \tag{3.65}$$

Substituting (3.65) into (3.59), the velocity of eddies is written as

$$v_l \sim \alpha^{\frac{1}{2}} (t_l \Omega_k)^{\frac{1}{2}} c_s \ . \tag{3.66}$$

3.4.3 The collisional velocity of dust grains in turbulent disks

Next we describe the collisional velocity of dust grains in turbulent disks according to Völk et al. (1980) and Weidenscilling (1984). Turbulence causes random motion of dust grains with the velocity $\sim v_L$. However, this random motion of them does not directly causes their collisional velocities. If all dust grains are well coupled to the turbulent motion of gas due to strong gas drag, the turbulence hardly enhance their collisional velocity. Hence, to evaluate their collisional velocity, we examine relative motion of dust grains to gas in turbulent motion.

The relative velocity is gorverned by the frictional time of dust grains given by $t_{\rm fric} = 1/(\Gamma\Omega_k)$. As mentioned above, the turbulent motion consist of various size of eddies. The period of the eddies t_l and the velocity v_l increase with the size l. Dust grains are tightly coupled to large eddis with $t_l \gg t_{\rm fric}$. Thus, such eddies does not enhance the relative velocity. For eddies with $t_l \lesssim t_{\rm fric}$, dust grains are not well coupled to the gas and such eddies can enhance the relative velocity of the grains. Among such eddies, the large ones (with $t_l \sim t_{\rm fric}$) have the largest velocity and, thus, the relative velocity of grains with $t_{\rm fric}$ is approximately given by thier velocity v_l. Substituting $t_l \sim t_{\rm fric}$ into equation (3.66), we have for the relative velocity $V_{\rm rel,t}$ by

$$V_{\rm rel,t} \sim \alpha^{\frac{1}{2}} \left(t_{\rm fric}\Omega_k\right)^{\frac{1}{2}} c_s \sim \left(\frac{\alpha}{\Gamma}\right)^{\frac{1}{2}} c_s. \tag{3.67}$$

At $z \leq H$, Γ is almost independent of the height z because the gas density is almost independent of the height z. Thus, the velocity of this eddy is almost independent of the height z. Small grains are well coupled to gas and have a very short frictional time. The periods of eddies have minimum value of $t_i \sim (\nu_{\rm mol}/\epsilon)^{1/2}$. Thus, for small dust grains with $t_{\rm fric} \lesssim t_i$, there are not eddies to which such dust grains are decoupled. In such a case, dust grains receive the accelaraion v_i/t_i and their relative velocity is given by

$$V_{\rm rel,t} \sim \frac{v_i}{t_i} t_{\rm fric} \ . \tag{3.68}$$

Using the obtained $V_{\rm rel,t}$, the collisional velocity of grains is approximately given by $(V_{\rm rel,t}^2 + V_r^2 + V_\phi^2 + V_z^2)^{1/2}$. However, at high altitude, collisional velocity is given by $(V_{\rm rel,t}^2 + V_z^2)^{1/2}$, because V_r and V_ϕ are much smaller than V_z. In Fig 5, we show the relative velocity $V_{\rm rel,t}$ at $z = H$ for various values of α. Here, V_z(solid line) is the vertical settling velocity. For $\alpha = 10^{-2}$, at size which the collisional velocity attain to the critical velocity (the hatched region), $V_{\rm rel,t}$ is larger than V_z. Thus, the collisional fragmentation is determined by $V_{\rm rel,t}$ for such aa large α. On the other hand, for $\alpha = 10^{-3}$, the collisional fragmentation is determined by V_z.

We show the relative velocity $V_{\rm rel,t}$ at $z = 0$ in Fig 6. Here, the solid line is the radial collisional velocity in laminar disks. For $\alpha > 10^{-4}$, when collisional fragmentation starts, $V_{\rm rel,t}$ is larger than V_r. Thus, the collisional fragmentation is determined by $V_{\rm rel,t}$ for $\alpha = 10^{-4}$ at the midplane.

3.4.4 Stirring-up of dust grains

The turbulence also stirs up dust grains, which presents them from settling. According to Mizuno (1989), we estimate the height to which dust grains are stirred up. The stirring-up due to the turbulence is described by the diffusion with the coefficient $\nu_{\rm turb}$. The diffusion time (or stirring-up time) is given by

$$t_{\rm diff} = \frac{z^2}{\nu_{\rm turb}} = \frac{z^2}{\alpha c_s H} = \frac{1}{\alpha \Omega_k}\frac{z^2}{H^2} \ . \tag{3.69}$$

On the other hand, the sedimentation time $t_{\rm settle}$ is given by

$$t_{\rm settle} = \frac{z}{V_z} = \frac{\Gamma}{\Omega_k} \ . \tag{3.70}$$

At the height to which dust grains are stirred up, $z_{\rm stir}$, the diffusion time (or stirring-up time) $t_{\rm diff}$ equals the sedimentation time $t_{\rm settle}$. Thus, we have for $z_{\rm stir}$

$$\frac{z_{\rm stir}}{H} = (\alpha\Gamma)^{\frac{1}{2}} \ . \tag{3.71}$$

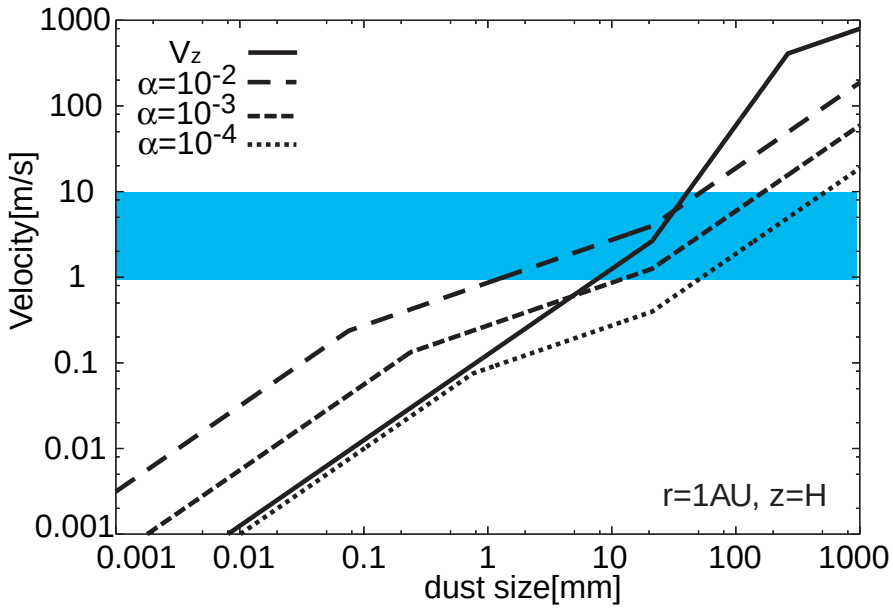

Figure 5: The velocity of the turbulent eddy. We show the relative velocity $V_{\rm rel,t}$ and V_z at r=1 AU, $z = H$. The solid line is the settling velocity V_z. The long dashed line, the short dashed line and the dotted line are $V_{\rm rel,t}$ for $\alpha = 10^{-2}, 10^{-3}$ and 10^{-4}, respectively. The hatched region shows the critical velocity (1-10 m/s).

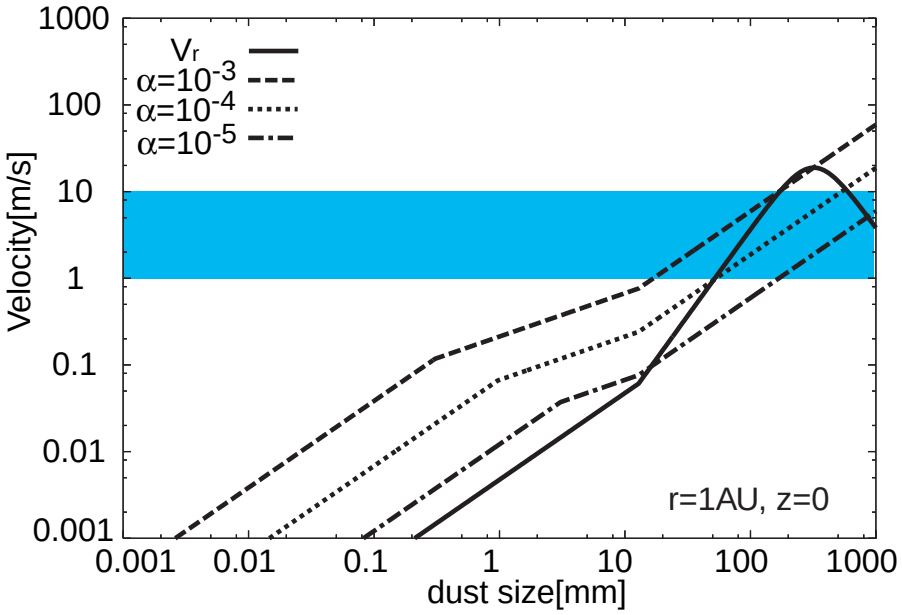

Figure 6: The velocity of the turbulent eddy. We show the relative velocity $V_{\rm rel,t}$ and V_r at r=1 AU, $z = 0$ (midplane). The solid line is the radial component of the collisional velocity V_r. The dashed line, the dotted line and the dash-dotted line are $V_{\rm rel,t}$ for $\alpha = 10^{-3}, 10^{-4}, 10^{-5}$, respectively. The belt shows the critical velocity ($1 - 10$ m/s).

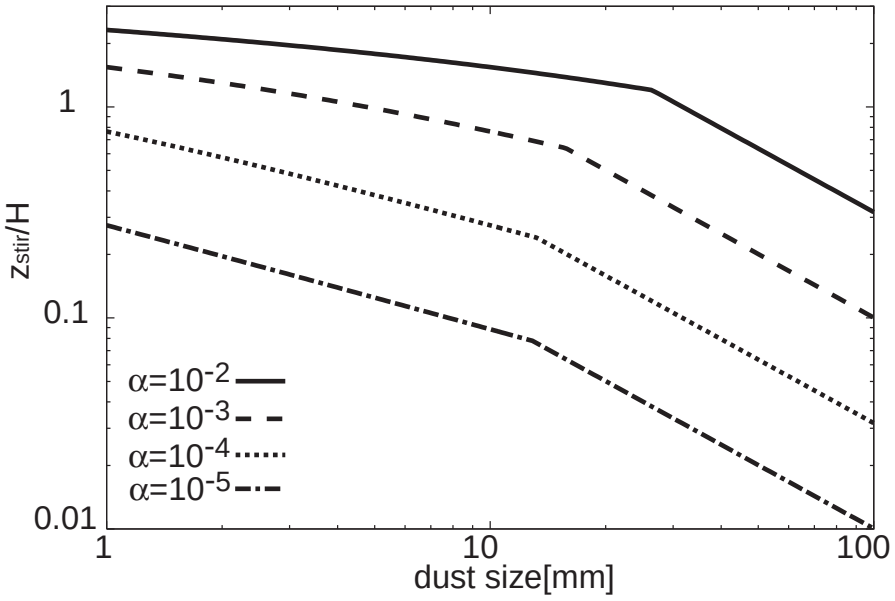

Figure 7: The height to where dust grains are stirred up at r=1 AU. The solid line, the dashed line, the dotted line and the dash-dotted line are $z_{\rm stir}$ for $\alpha = 10^{-2}, 10^{-3}, 10^{-4}, 10^{-5}$, respectively.

Above $z = z_{\rm stir}$, the $t_{\rm settle}$ is shorter than $t_{\rm diff}$ and the sedimentation is dominant while the stirring-up is dominant below $z_{\rm stir}$. Takeuchi and Lin (2002) examined the height to which dust grains are stirred up more exactly. Their result is almost consistent with our estimation for the case of $z_{\rm stir} \lesssim H$ We show the height $z_{\rm stir}$ in Fig 7. As turbulence becomes weak (α decreases), $z_{\rm stir}$ decreases. For $\alpha \geq 10^{-2}$ dust grains with $a \simeq 1$ mm are stirred up to $z > 2H$. Substituting equation (3.71) into (3.37), the velocity of dust grains at high altitude is written as

$$V_{\rm col} \simeq V_z = -\frac{1}{\Gamma}\frac{z}{r}v_k = -\left(\frac{z}{z_{\rm stir}}\right)^{\frac{1}{2}} V_{\rm rel,t} \ . \tag{3.72}$$

Hence, at $z = z_{\rm stir}$, $|V_z| = V_{\rm rel,t}$. This is because at $z = z_{\rm stir}$, the acceleration $V_{\rm rel,t}/t_{\rm fric}$ by the coupling eddies equals the vertical component of the gravity of the centrals star, $\Omega_k^2 z$. The

collisional velocity $V_{\rm col}$ is given by

$$V_{\rm col} = (V_{\rm rel,t}^2 + V_r^2 + V_\phi^2 + V_z^2)^{1/2} \ . \tag{3.73}$$

At $z > z_{\rm stir}$, the collisional velocity is the same as in laminar disk:

$$V_{\rm col} \simeq \frac{1}{\Gamma}\frac{z}{r} \ . \tag{3.74}$$

At the region with $z \lesssim z_{\rm stir}$, where dust grains exist, $V_{\rm rel,t}$ is comparable with or larger than V_z. The collisional velocity is given in turbulent disks by

$$V_{\rm col} \simeq \left(\frac{\alpha}{\Gamma}\right)^{\frac{1}{2}} c_s \ . \tag{3.75}$$

In the case with $z_{\rm stir} \lesssim H$, the collisional velocity of equation (3.75) is independent of z, because Γ is independent of z at $z \lesssim H$.

4 The collisional velocity in the course of the dust growth

The fragmentation occurs at the mutual collisions of grains, if the internal pressure enhanced by the collision is larger than the tensile strength of the grains. This collisional fragmentation would prevent the dust growth. In previous section, we obtained the collisional velocity $V_{\rm col}(a, r, z)$ for various grain size at each place. In this section, we examine the maximum size to which dust grains attain in the course of the dust growth and evaluate their collisional velocity and the effects of collisional fragmentation.

4.1 The dust growth in laminar disk

In laminar disks, the collisional velocity is given by (3.35), (3.36), (3.37) and (3.45). We examine the growth of dust grains and obtain the collisional velocity in the course of the dust growth.

4.1.1 Analytical estimation of dust growth

First, we analytically estimate the maximum size to which dust grains grow during their settling. Safronov (1969) estimated the maximum size of the dust grains, assuming large grains collide with only floating small grains and solving growth of large grains. Tanaka et al. (2005) also estimated the maximum size in a simpler way. They assumed that after the settling time of dust becomes equal to the growth time, dust grains settle without further growth. The settling time $t_{\rm settle}$ is given by equation (3.70). The growth time is given by

$$t_{\rm grow,z} = \frac{a}{\dot{a}} = \frac{3}{p_s \bar{n} \sigma_{m,m} V_{\rm col}} \ , \tag{4.1}$$

where $\bar{n}$ is the grain number density, p_s is the sticking probability and $\sigma_{m,m}$ the collisional cross section between grains with masses m and m'. Here, $\bar{n}$ is given by $\zeta_d \rho_g / m$ and $\sigma_{m,m} = \pi(2a)^2$. At high altitude, the collisional velocity is given by $V_{\rm col} = V_z$. Thus, $t_{\rm grow,z}$ is written as

$$t_{\rm grow,z} = \frac{\rho_{\rm mat}}{p_s \zeta_d \rho_g} \frac{a}{z} \frac{\Gamma}{\Omega_k} \ . \tag{4.2}$$

The maximum size that the dust grains grow in the settling process $a_{\rm settle}$ is defined by $t_{\rm settle} = a_{\rm grow,z}$. Thus $a_{\rm settle}$ is given by

$$a_{\rm settle} = \frac{p_s \zeta_d}{\sqrt{2\pi e}} \frac{\Sigma_g}{\rho_{\rm mat}} \ . \tag{4.3}$$

This maximum size is almost consistent with that obtained by Safronov (1969).

4.1.2 Numerical calculation of dust growth

The above analytical estimate of the maximum size of settling grains would have some error. To obtain more accurate maximum size. We perform numerical simulations fo dust growth and settling in the same way as Tanaka et al. (2005). We briefly describe their basic equation an numerical procedure. The statistical coagulation equation is used to describe evolution of the mass distribution due to collisional growth. To describe dust settling, a

vertical advection term is added to the coagulation equation. That is, the following equation is used:

$$\begin{aligned}&\frac{\partial}{\partial t}n(m,z)+\frac{\partial}{\partial z}\left[V_z n(m,z)\right]\\&=\frac{1}{2}\int_0^m K_{m',m-m'}n(m',z)n(m-m',z)dm'\\&\quad-n(m,z)\int_0^\infty K_{m,m'}n(m',z)dm'\ ,\end{aligned}\tag{4.4}$$

where the kernel, $K_{m',m-m'}$, is related to the coalescence rate between grains with masses m and $m-m'$. In this equation, the first term on the right-hand side indicates the formation of grains of the mass m by collisions between the smaller grains, and the second term represents the consumption of grains with the mass m as a result of collisions with other grains. The second term on the left-hand side is the advection term, which describes the vertical mass transport. In equation (4.4), the advection term due to the radial mass transport is neglected because it is effective only for relatively large grains that settle down to the dust layer.

The kernel $K_{m',m-m'}$ is given by $p_s\sigma_{m,m'}\Delta V_{m,m'}$, where $\sigma_{m,m'}$ is the collisional cross section between grains with masses m and m', p_s is the sticking probability, and $\Delta V_{m,m'}$ is the relative velocity between grains with m and m'. For dust grains, $\sigma_{m,m'}$ is equal to the geometrical cross section. We assume spherical grains in this study. Then we obtain the cross section $\sigma_{m,m'}$ as $\pi[a(m)+a(m')]^2$, where $a(m)$ is the radius of grains with m. Because we neglected the radial drift of grains, equation (4.4) can be integrated at each radial position independently.

We adopt the numerical method of Tanaka et al. (2005). Equation (4.4) is integrated with respect to time with first-order accuracy. The change in the number density $n(m,z)$ due to coagulation which comes from two terms on the right-hand side of equation (4.4) calculated with the fixed bin scheme (Nakagawa et al. 1981, Ohtsuki et al. 1990). The representative masses, m_k, of the smallest six bins are set to be km_0 ($k \leq 6$). The larger mass bins are spaced logarithmically with a multiplication factor 1.15 (i.e., $m_k = 1.15m_{k-1}$). The change due to

the advection term which comes from the second term on the left-hand side. To calculate it accurately and stably, we used the spatially third-order MUSCL-type (Monotonic Upwind Scheme for Conservation Law-type) scheme developed by van Leer (1977).

As an initial condition for numerical calculations, all grains have the radius of 0.1μm initially. We assume the dust-to-gas ratio is uniform initially. The density and the temperature of the disk are not varied with time during numerical simulations for simplicity.

In the numerical integration of equation (4.4), the z-axis from $z = 0$ to $z = 2.5\sqrt{2}H$ is divided into 251 equally spaced grids at each radial position. As for the coordinate of the grain mass, we divide it into 500 discrete fixed mass bins. The minimum mass bin is that of grains with the radius of 0.1 μm, and its representative mass, m_0, is $4\pi\rho_{\rm mat}(0.1\mu{\rm m})^3/3$.

We show the obtained mass distribution at $r = 1$AU and $z = H$ in Figure 8. At first ($t < 150$yr), the size distribution of dust grains has one peak. In this stage, the peak size of the distribution increases with time (i.e., grains grow) and the settling is negligible. At t=150yr, on the other hand, the size distribution has two peaks. The left peak (at a smaller) indicates that dust grains which grow at $z = H$. The right peak (at larger) indicates that dust grains settling from the higher level ($z > H$). The large dust grains settle earlier than the small ones. At t=300yr, the peak size decreases. This is because large grains settle down and only the smaller ones remains at $z = H$. Thus, when the size distribution has two peaks, the dust size becomes maximum. In the numerical results, we define the maximum size by the left peak size of the distribution.

Figure 9 shows the analytical results (solid line) and the numerical results (points) of $a_{\rm settle}$ at r=1AU. The numerical results shows that the maximum size depends on z/H and that dust grains further grow during the settling stage. This is because the density of dust grains is enhanced at the lower layer ($z \simeq 0.1H$). The numerical results agree well with the analytical results at lower layer. Thus, the collision rate is large and the growth time is short at lower layer. The sedimentation time is almost independent of z/H. Thus, the

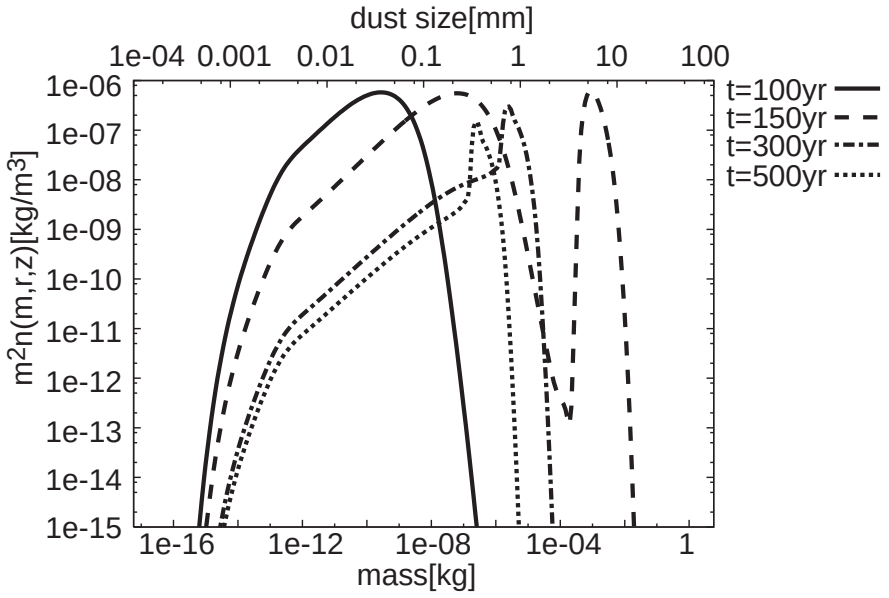

Figure 8: Time evolution of grains size distributions at $r = 1$ AU, $z = H$. The solid line, the dashed line, the dashed-dotted line and the dotted line are the size distribution of dust grains in $t = 100$ yr, $t = 150$ yr, $t = 300$ yr and $t = 500$ yr ,respectivsely.

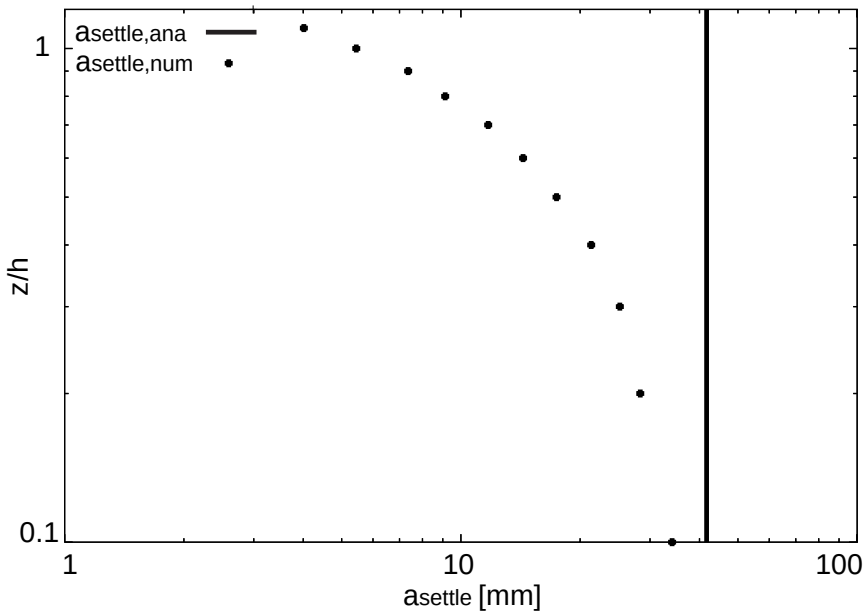

Figure 9: The maximum dust size $a_{\rm settle}$ at each height. The points show the numerical results. The solid line shows the analytical results.

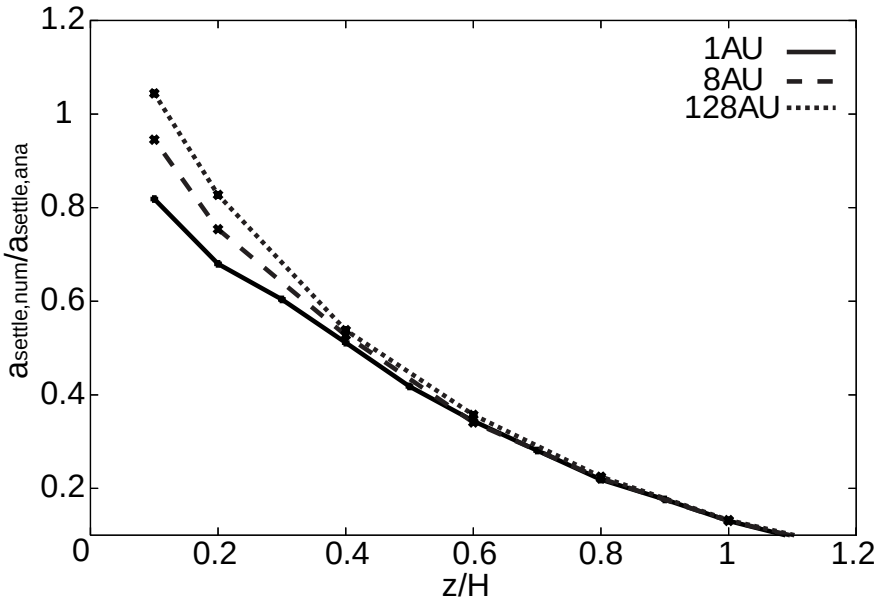

Figure 10: The ratio of numerical results $a_{\mathrm{settle,num}}$ to analyrical estimations $a_{\mathrm{settle,ana}}$. The solid line, the dashed line and the dotted line are $a_{\mathrm{settle,num}}/a_{\mathrm{settle,ana}}$ in $r = 1$ AU, $r = 8$ AU and $r = 128$ AU respectively.

maximum size that the dust grains grow $a_{\rm settle}$ is large at lower layer. The ratio of the numerical result $a_{\rm settle,num}$ to the analytical one $a_{\rm settle,ana}$ is shown in Figure 10. This ratio is almost independent of the distance from the central star r.

We also examine $a_{\rm frag}$ through the numerical calculation. We assume that when the collisional velocity $V_{\rm col}$ is larger than $V_{\rm frag}$, dust grains do not grow (the sizes do not change) in the collision. We show the obtained mass distribution at $r = 1$AU and $z = H$ for $V_{\rm col} = V_{\rm frag}$ in Figure 11. At first ($t < 300$yr), the peak size of the distribution increases with time and the settling is negligible. At t=500yr, the peak size decreases. This is because large grains settle down and only the smaller ones remains at $z = H$. Thus, the peak size has the maximum value when the peak size starts to decrease. In the numerical results, we define the maximum size by the peak size of the distribution ($\sim$ 1 mm). The growth of dust grains in the fragmentation case has same tendency of the non-fragmentation case (see Figure 8 and 11). However, the growth time in the fragmentation case is larger than one in the non-fragmentation case. Thus, the maximum dust size is smaller than ones (e.g., $a_{\rm settle}$) in the non-fragmentation case. Consequently, the settling time is also longer than one in the non-fragmentation case. In this case, the dust growth stops at $z = H$ before dust grains start to settle at higher altitude ($z < H$). Thus, the dust growth at $z = H$ makes a peak before the dust settling at higher altitude makes a peak. Then, because two peak sizes are comparable, the size distribution has only one peak. Figure 4 shows the numerical results and the analytical estimation of $a_{\rm frag}$. The ratio of analytical estimations to numerical results is $0.5 - 2$. The analytical estimations are consistent with the numerical results.

4.1.3 The effects of collisional fragmentation on dust growth and settling

Finally, we examine where collisional fragmentation occurs at high altitude. When dust grains collide each other, if the pressure due to the collision is larger than the tensile strength, the collisional fragmentation occurs. That is, when the collisional velocity $V_{\rm col}$ is larger than

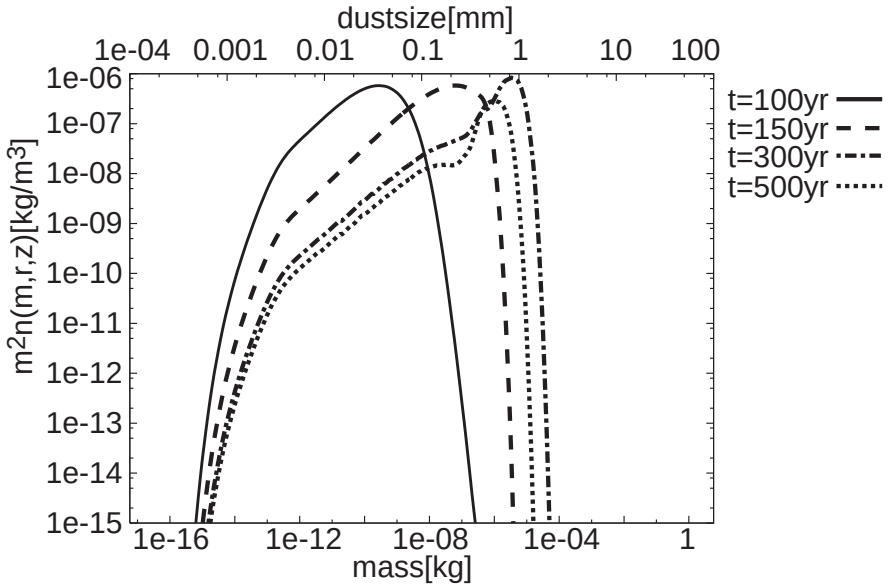

Figure 11: Time evolution of grains size distributions for $V_{\rm frag} = 1$ m/s at $r = 1$ AU, $z = H$. The solid line, the dashed line, the dashed-dotted line and the dotted line are the size distribution of dust grains in $t = 100$ yr, $t = 150$ yr, $t = 300$ yr and $t = 500$ yr ,respectivsely.

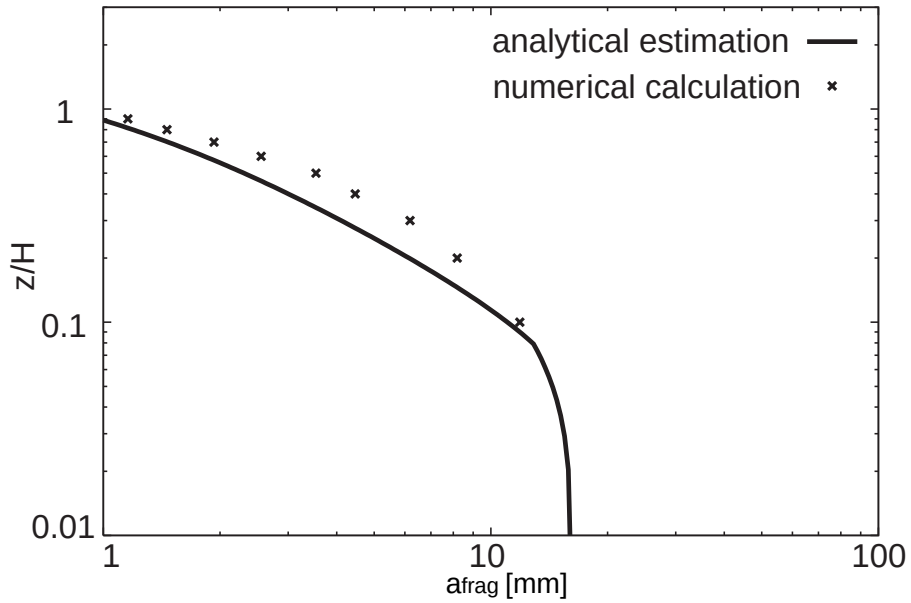

Figure 12: The solid line and the points are the analytical estimation and the numerical results of $a_{\rm frag}$ for $V_{\rm frag} = 0.1$m/s at $r = 1$ AU , respectively.

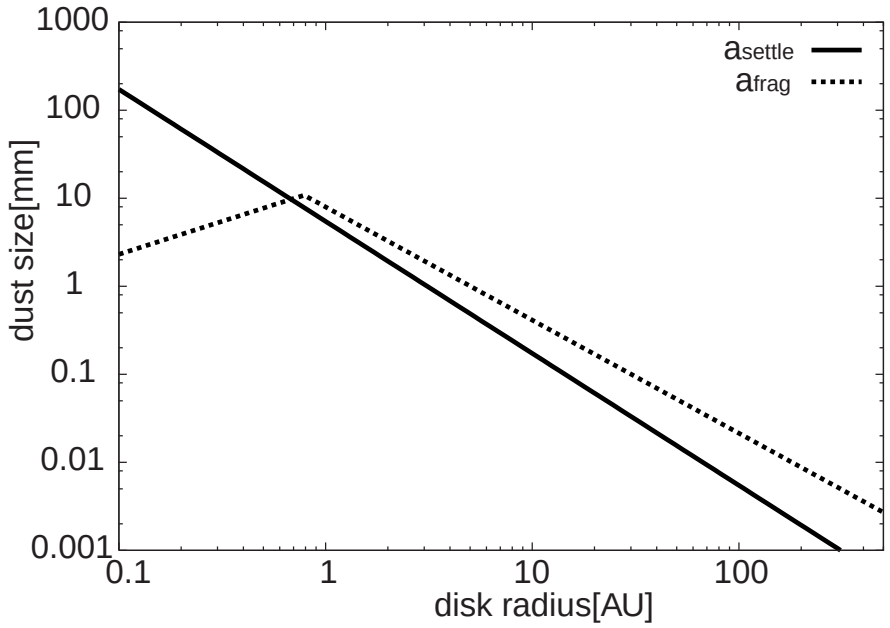

Figure 13: The maximum dust size $a_{\rm frag}$ and $a_{\rm settle}$ at $z = H$ and r=1 AU. The solid line is $a_{\rm settle}$. The dashed line is $a_{\rm frag}$ for $V_{\rm frag} = 1{\rm m/s}$.

the critical velocity $V_{\rm frag}$.

As dust grains grow, the velocity increases. Thus, the growth of the large dust grains is prevented by collisional fragmentation. However, large dust grains have the large settling velocity. Dust grains with $a > a_{\rm settle}$ settle before they futher grow. Thus, if $a_{\rm settle}$ is smaller than $a_{\rm frag}$, collisional fragmentation does not occur and the maximum dust size is determined by $a_{\rm settle}$. On the other hand, when $a_{\rm frag}$ is smaller than $a_{\rm settle}$, collisional fragmentation occurs.

We show $a_{\rm frag}$ and $a_{\rm settle}$ in Figure 13. At inner region ($r \lesssim 1$AU), $a_{\rm frag}$ is larger than $a_{\rm settle}$. Thus, the maximum dust size is determined by collisional fragmentation at inner region. On the other hand, at outer region ($r \gtrsim 1$AU), $a_{\rm frag}$ is smaller than $a_{\rm settle}$. Thus, the maximum dust size is determined by sedimenation at outer region. In another way, if the

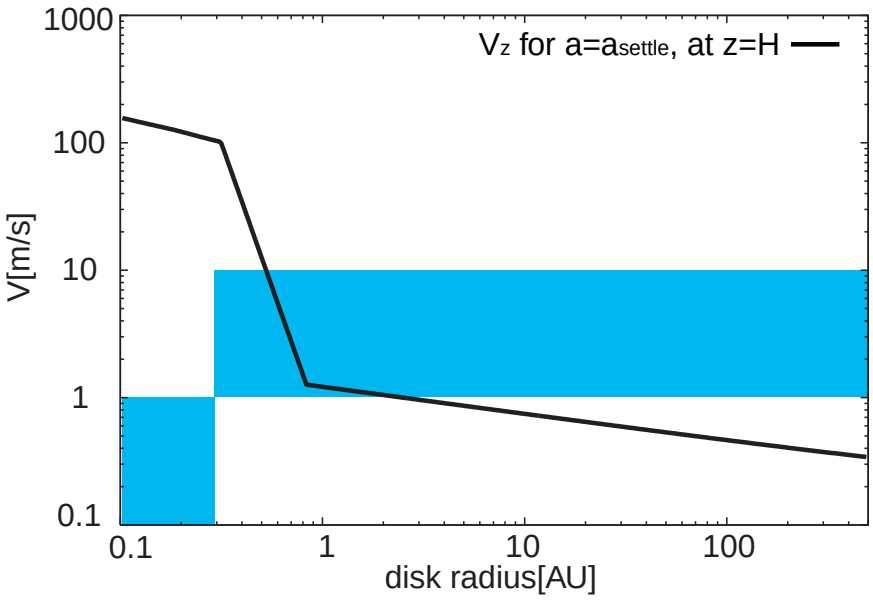

Figure 14: The collisional velocity for $a = a_{\rm settle}$ at $z = H$. The solid line is the collisional velocity for $a = a_{\rm settle}$ at $z = H$. The belt shows the critical velocity $V_{\rm frag}$. The critical velocity is 1-10 m/s at $r \lesssim 0.4$ AU (H_2O ice do not evaporate) and it is 0.1-1 m/s at $r \gtrsim 0.4$ AU (H_2O ice evaporate).

collisional velocity of dust grains with $a = a_{\rm settle}$ is larger than the critical velocity, collisional fragmentation occurs.

The collisional velocities of dust grains with $a = a_{\rm settle}$ at high altitude ($z = H$) are written as follows:

For Epstein's law ($a_{\rm settle} \leq \frac{3}{2} l_g$), the collisional velocity is given by

$$V_{\rm col} = -\sqrt{\frac{\pi}{8}} p_s \zeta_d c_s \ . \tag{4.5}$$

For Stokes' law ($a_{\rm settle} > \frac{3}{2} l_g$), the collisional velocity is given by

$$V_{\rm col} = -\frac{1}{\sqrt{72\pi}e} \frac{\sigma_{col}(p_s \zeta_d \Sigma_g)^2}{\mu m_\mu \rho_{mat} H} c_s \ . \tag{4.6}$$

For $\mathcal{R} > 100$ the collisional velocity is given by

$$V_{\rm col} = \sqrt{\frac{8}{3}\frac{p_s \zeta_d}{C_D}} c_s \ . \tag{4.7}$$

This collisional velocity depends on the dust-to-gas ratio ζ_d. The gas drag force is proportional to gas density ρ_g. The maximum dust size $a_{\rm settle}$ is proportional to dust density ρ_d. The collisional velocity depends on the gas drag force and the maximum dust size $a_{\rm settle}$. Thus, the collisional velocity of the maximum dust grain depends on the dust-to-gas ratio ζ_d. This collisional velocity depends on the dust-to-gas ratio ζ_d and the sound speed c_s. Thus, the disk model dependence of our results is only the dust-to-gas ratio ζ_d and the sound speed c_s. We show the collisional velocity with $a = a_{\rm settle}$ in Figure 14. At $r < 0.4$ AU ($T < 150$ K) H_2O ice do not evaporate and the surface of dust grains is H_2O ice. Thus, the tensile strength is large and the critical velocity is large. In this region the critical velocity is $V_{\rm frag} = 1 - 10$ m/s. On the other hand, at $r > 0.4$ AU ($T > 150$ K) H_2O ice evaporate and the surface of dust grains is SiO_2. Thus, the tensile strength is small and the critical velocity is small. In this region the critical velocity is $V_{\rm frag} = 0.3 - 1$ m/s. At inner region ($r \lesssim 1$AU), the collisional velocity is larger than the critical velocity. At high alititude ($z = H$), collisional fragmentation occurs at inner region ($r \lesssim 1$AU) only.

Finally, we examine the effects of collisional fragmentation on dust growth and settling. The maximum dust size is determined by $a_{\rm settle}$ and $a_{\rm frag}$ in the course of the dust settling.

Figure 15 shows $a_{\rm settle}$ (solid line) and $a_{\rm frag}$ (dashed line) at 1 AU. In Figure 15, $a_{\rm frag}$ is comparable with $a_{\rm settle}$. Thus, collisional fragmentation does not occur in the course of the dust settling at $r = 1$ AU. On contrast, Figure 16 shows $a_{\rm frag}$ (solid line) and $a_{\rm settle}$ (dashed line) at $r = 0.5$ AU. At high altitude ($z \gtrsim H$), $a_{\rm settle}$ is smaller than $a_{\rm frag}$. Then, dust grains grow along $a_{\rm settle}(z)$ (dashed line). After $a_{\rm settle} = a_{\rm frag}$, collisional fragmentation occurs and the dust growth stops. However, as dust grains settle (z decreases), the collisional velocity (the settling velocity) decreases. Then dust grains can grow. Dust grains settle and grow along $a_{\rm frag}(z)$ (solid line). In the course of the dust settling, collisional fragmentation occurs

at inner region. At near the midplane ($z \lesssim 0.1\ H$), $a_{\rm frag}$ is almost independent of z. Then the dust growth stops. That reason is that the collisional velocity is given by the radial velocity V_r and it is almost independent of z. The height where $a_{\rm frag}$ saturates is consistent with the height where is defined by $V_z = V_r$ (equation (3.51)). After dust grains settle below $z \simeq 0.1\ H$, dust grains settle without further grow.

4.2 The effects of collisional fragmentation on dust growth in turbulent disks

In this section, we examine the effects of collisional fragmentation on dust growth and settling in turbulent disks. In laminar disks, as dust grains settle, the collisional velocity decreases and $a_{\rm frag}$ increases. IN turbulent disks, at $z > z_{\rm stir}$, the stirring-up is not effective and the collisional velocity is given by equation (3.37) or (3.35) as laminar disks, when dust grains settle down to $z = z_{\rm stir}$, they cannot settle more. We show $a_{\rm frag}$ and $z_{\rm stir}$ in Fig. 17. The damping time of turbulence would be much longer than the dust sedimentation timescale. Thus, dust grains settle very slowly and grow along $a_{\rm frag}(z)$. The size $a_{\rm settle}$ is meaningless in this case. At $z < z_{\rm stir}$, the collisional velocity is given by $V_{\rm rel,t}$ (equation (3.75)). However, collisional fragmentation mainly occurs at $z < z_{\rm stir}$, because $V_{\rm rel,t}$ is smaller than $V_z(z = z_{\rm stir})$.

5 Summary and Discussion

In this paper, we clarified the region where collisional fragmentation occurs in laminar disks or turbulent disks and examine the effects of collisional fragmentation on dust growth. Our results are summarized as follows:

1. Collisional fragmentation occurs, when the internal pressure $P_{\rm col}$ enhanced by the collision is larger than the tensile strength Y of the grains. Such a high pressure is

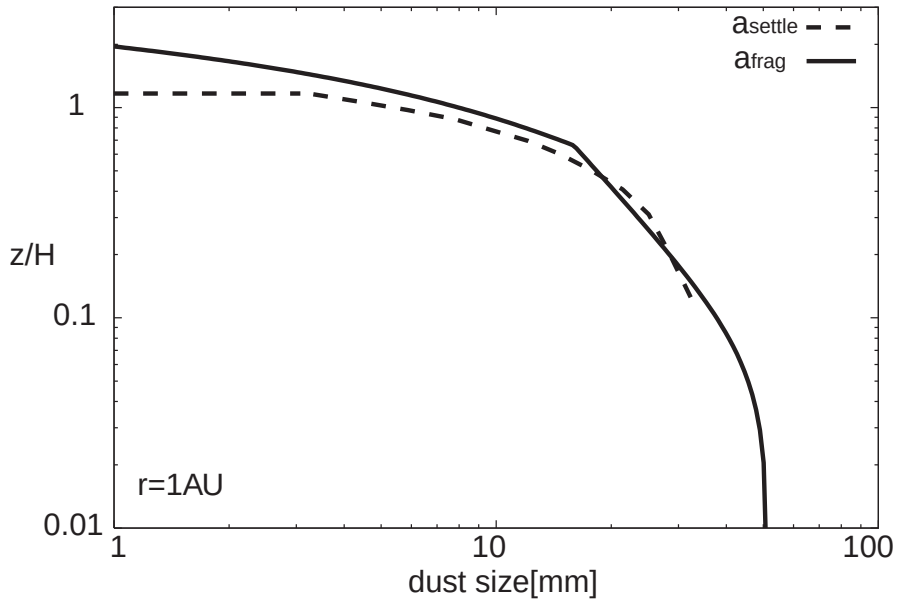

Figure 15: The settling and growth of dust grains at $r = 1$ AU in the laminar disk. The solid line is $a_{\rm frag}$ for $V_{\rm frag} = 1$m/s and the dashed line is $a_{\rm settle}$ at $r = 1$ AU.

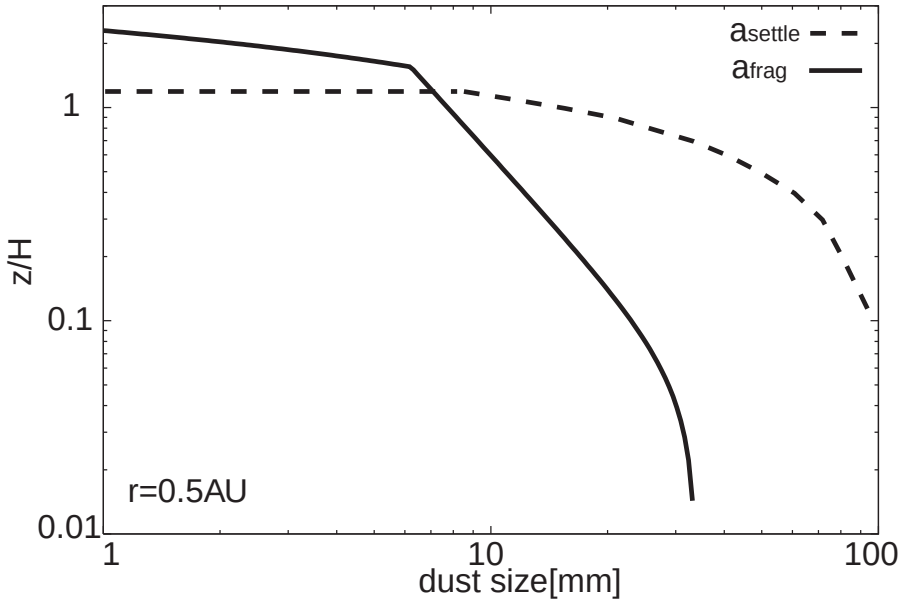

Figure 16: The settling and growth of dust grains at $r = 0.5$ AU in the laminar disk. The solid line is $a_{\rm frag}$ for $V_{\rm frag} = 1$m/s and the dashed line $a_{\rm settle}$ at $r = 0.5$ AU.

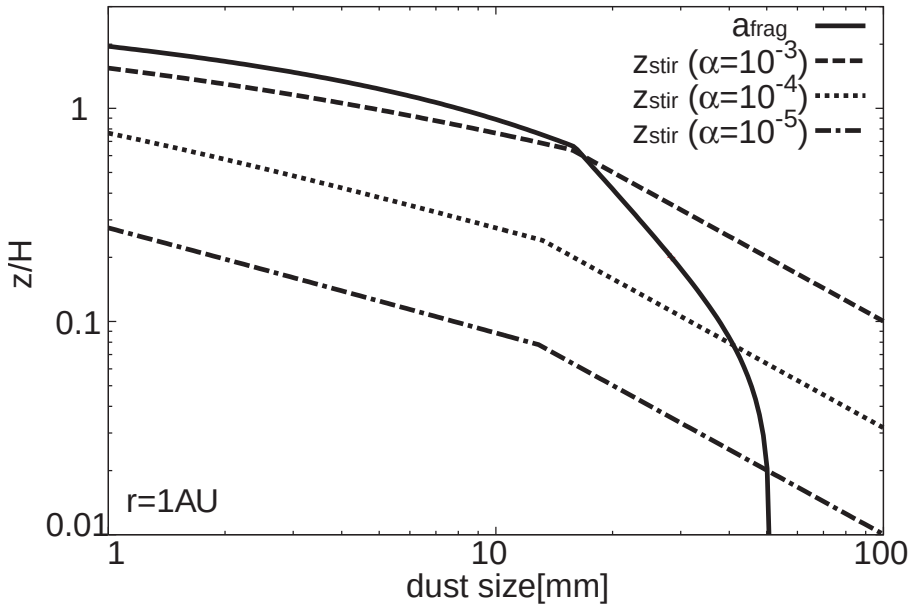

Figure 17: The settling and growth of dust grains at $r = 1$ AU in the turbulent disk. The long dashed line, the short dashed line and the dotted line are $a_{\rm frag,t}$ for $\alpha = 10^{-2}, 10^{-3}, 10^{-4}$, respectively. The solid line is $a_{\rm frag}$ for $V_{\rm frag} = 1{\rm m/s}$ at $r = 1$ AU. The dashed lines are $z_{\rm stir}$ for $\alpha = 10^{-3}, 10^{-4}, 10^{-5}$, respectively.

realized when the collisional velocity is larger than a certain critical velocity determined by the strength Y. The strength of dust grains is governed by an adhesion force between monomers. Using the JKR theory and assuming compact dust grains consisted of sub-micron monomers, we estimated the tensile strength Y (equation (2.2) or Sirono and Greenberg 2000) and estimated the critical velocity $V_{\rm frag}$ (equation (2.6)). That is, the critical velocity is 3 m/s for H_2O grains and 0.3 m/s for SiO_2 grains. Detail numerical simulations of aggregate collision done by Dominik and Tielens (1997) and the collision experiments by Blum and Wurm (2000) indicate that the critical velocity is larger than our estimate by the factor 3. On the other hand, if porous grains are consisted, the critical velocity would be much smaller than our estimation. To fix the critical velocity for fragmentation more accurately, further investigation on grain structure is needed.

2. The collisional velocities between grains are approximately given by the relative velocities between grains and gas, which increases with the grain mass as long as thier frictional time is smaller than the Keplerian period. In the course of dust growth, the collisional velocity increases. If the collisional velocity attains to the critical one, collisional fragmentation occurs and prevents further dust growth.

3. In laminar disks, the collisional velocity $V_{\rm col}$ is given by the settling velocity V_z (equation (3.37)) during dust settling and by the radial V_r near the midplane of disks. Using this collisional velocity, we also obtained the dust size, $a_{\rm frag}(z)$ (equation (3.54), (3.55)), for which $V_{\rm col}$ equals the critical velocity. On the other hand, we also obtain the maximum size to which grains grow before settling, $a_{\rm settle}$(z), analytically or numerically (equation (4.3)). If the critical size for fragmentation $a_{\rm frag}$ is smaller than $a_{\rm settle}$, fragmentation inhibits dust growth during settling. This condition is satisfied at $r \lesssim 1$ AU in the minimum-mass nebula disk around a solar type star. As dust grains settle, the collsional velocity decreases and they can grow more (see figure 16).

At the midplane, the collisional velocity is given by the radial velocity V_r (equation (3.35)). The radial velocity attains its maximum value at the size with $\Gamma(a) = 1$ (see figure 3). The maximum velocity is given by $\eta v_k \simeq 20$ m/s for Kusaka model and 50 m/s for Hayashi model, which is larger than the critical velocity ($\lesssim 10$ m/s). Thus, collisional fragmentation wouled inhibit dust growth at the midplane of the whole disks and the maximum dust size is given by $a_{\rm frag}(z = 0)$ (equation (3.54) or (3.55)). The ratio of $V_{\rm frag}/\eta V_k$ is very important in the dust growth and planetesimal formation. The uncertainly of $V_{\rm frag}$ still remains. If $V_{\rm frag}$ is larger than ηV_k, dust grains can grow more and they are able to be decoupled with the disk gas, which would help the gravitational instability of dust layer.

4. For turbulent disks, we considered homogneous and isotropic turbulence and adopted the so-called α-model. There are two effects of turbulence on the dust growth and settling. One is the enhancement of the collisional velocity due to turbulent motion. The other one is the vertical diffusion of dust grains. In strong turbulent disks ($\alpha > 10^{-2}$), the collisional velocity is given by $V_{\rm rel,t}$ (equaiton (3.67)) while in weak turbulent disks ($\alpha < 10^{-2}$), the collisional velocity is given by V_z or V_r as laminar disks. Dust grains are stirring up to $z = z_{\rm stir}$ (equaiton (3.71)) in turbulent disks. At a higher level ($z > z_{\rm stir}$), grains settle down and the collisional velocity is given by V_z (equation (3.37)) as laminar disks. On the other hand, grains cannot remain at $z < z_{\rm stir}$. The settling velocity is comparable to $V_{\rm rel,t}$, at $z \sim z_{\rm stir}$. The maximum dust size to which dust grains can grow is given by $a_{\rm frag}(z = z_{\rm stir})$. As disk turbulence damps (α decreases), $z_{\rm stir}$ and the collisional velocity decreases and dust grains gradually settle and grow (see figure 17).

Collisional fragmentation also confines dust migration in the disks. This is because the relative velocity of dust grains to the disk gas depends on the dust size and the dust size is confined by collisional fragmentation. As a result, the relative velocity of grains to the

disk gas is limited to the critical velocity for fragmentation $V_{\rm frag}$, which is not depending on the disk model but only on the properties of dust grains. It should be noticed that this limitation on dust migration works only when the collisional frequency between grains is so high that the collisional fragmentation can regulate the dust size.

For example, we can estimate the radial migration time of dust grains in gas disks $t_{\rm mig}$ to be $r/V_{\rm frag}$. If we adopt $V_{\rm frag} = 3$ m/s, the radial migration time is obtained as 2×10^5 yr. Because the collisional time of grains in the minimum-mass nebula disk is much shorter than $t_{\rm mig}$, the collisional fragmentation is frequent enough to regulate the dust size. Hence, in this time scale of $t_{\rm mig}$, small grains created by fragmentation also remain in whole disk. The critical velcoity $V_{\rm frag}$ can be much larger than the above value. Some authors obtained mush shorter dust radial migration time, considering the meter-sized particle (e.g., Cuzzi et al 2004). Such a rapid migration is excluded if collisional frgmentation is taken into account.

Another example is the concentration of dust grains trapped in turbulent eddies. Some authors suggested that dust migration in anticyclonic eddies enhances that dust density and could even trigger a local gravitational instability (e.g., Barge and Sommeria 1995). Tanga et al (1996) showed that large-scale vortices may be naturally generated in a differentially rotating solar nebula. The dust-trapping efficiency of vortices was explored analytically by Chavanis (2000) for vortices of arbitrary aspect ratio. Johansen et al. (2004) performed the simulations of dust-trapping eddies. According to their result, the lifetime is a few times as long as the Keplerian period when the eddy size is the disk scale height. In most studies, the lifetime of eddies is estimated to be order of the Keplerian period and a very high migration velocity of dust is needed to pile up dust grains within the lifetime. Such a rapid migration is also excluded because of collisional fragmentation. In order to concentrate the dust grains under the limitation of collisional fragmentation, eddies with much longer lifetime is needed.

As mentioned above, collisional fragmentation affects the evolution of dust grains (e.g., the dust growth, settling and migration). Thus, the critical velocity $V_{\rm frag}$ is the very im-

portant parameter. However, there is uncertainty the critical velocity. In this study, we considered compact spherical dust grains (aggregates). However, coagulation of dust grains produce aggregates that have highly irregular shapes and high porosity (Meakin and Donn 1988, Weidenschilling and Cuzzi 1993). Wurm and Blum (1998) experimentally studied the mass evolution of a dust grains embedded in a rarefied turbulent gas environment. According to their results, for $a \lesssim 1$ μm and $V_{\rm col} \lesssim 0.1$ m/s the dominant growth process is due to collisions between aggregates of very similar sizes. This process produces high porosity aggregates. Blum and Scräpler (2004) measured the tensile strength of high-porosity dust aggregates. The obtained tensile strength is $\sim$1000 Pa and it is much smaller than the analytical estimated value $\sim$ 30000 Pa. Thus, the critical velocity may be much smaller than the estimated value 0.3 m/s. On the other hand, the velocity for high porosity aggregates is also different from the velocity for compact aggregates because the ratio of mass to the cross section is not proportional to the radius. Consequently, the size dependence of the velocity for high porosity aggregates is different from ones for compact aggregates. To investigate the growth of high porosity aggregates, it is important that clarify the structure of the aggregates (e.g., the strength and the relation between the mass and the radius).

Acknowledgements

I gratefully acknowledge to Hidekazu Tanaka for the teaching. I thank to Koji Wada for the comments about fragmentation. I also thank to the menbers of ice and planetary group, Institute of Low Temperature Science and the menbers of ida labolatory for helpful suggestions.

References

Adachi, I., C. Hayashi, and K. Nakazawa 1976. The gas drag effect on the elliptical motion of a solid body in the primitive solar nebula. *Prog. Press, Phys.* **56**, 1756-1771.

Barge, P., and J. Sommeria 1995. Did planet information begin inside presistent gaseous vortices? *Astron. Astrophys.* **295**, L1-L4.

Blum, J., and R. Schräpler 2004. Structure and mechanical properties of high-porosity macroscopic agglomerates formed by random ballistic deposition. *Phy. Rev. Lett.* **93**, 115503.

Blum, J., and G. Wurm 2000. Experiments on sticking, restructuring, and fragmentation of preplanetary dust aggregates. *Icarus* **143** 138-146.

Cuzzi, J. N., and K. J. Zahnle 2004. Material Enhancement in protoplanetary nebulae by particle drift through evaporation Fronts. *Astrophys. J.* **614** 490-496,

Chavanis, P. H. 2000. Trapping of dust by coherent vortices in the solar nebula *Astron. Astrophys.* **356**, 1089-1111.

Chokshi, A., A. G. G. M. Tielens, and D. Hollenbach 1993. Dust coagulation. *Astrophys J.* **407**, 806-819.

Dominik, C., and A. G. G. M. Tielens 1995. Resistance to rolling in the adhesive contact of two spheres. *Phil. Mag. A* **72**, 783-803.

Dominik, C., and A. G. G. M. Tielens 1996. Resistance to rolling on atomic scales in the adhesive contact of two elastic spheres. *Phil. Mag. A* **73**, 1279-1302.

Dominik, C., and A. G. G. M. Tielens 1997. The physics of dust coagulation and the structure of dust aggregates in space. *Astrophys. J.* **480**, 647-673.

Dullemond, C. P., and C. Dominik 2004. The effect of dust settling on the appearance of protoplanetary disks *Astron. Astrophys.* **421**, 1075?1086.

Dullemond, C. P., and C. Dominik 2005. Dust coagulation in protoplanetary disks: A rapid depletion of small grains *Astron. Astrophys.* **434**, 971-986.

Heim, L-. O., J. Blum, M. Preuss, and H. J-. Butt 1999. Adhesion and friction forces between spherical micrometer-sized particles. *Phys. Rev. Lett.* **83**, 3328-3331.

Goldreich, P., and W. R. Ward 1973. The formation of planetesimals. *Astrophys. J.* **183**, 1051-1061.

Hayashi, C. 1981. Structure of the solar nebula, growth and decay of magnetic fields, and effects of magnetic and turbulent viscosities on the nebula. *Progr. Theor. Phys. Suppl.* **70**, 35-53.

Johnson, K. L., K. Kendall, and A. D. Roberts 1971. Surface energy and the contact of elastic solids. *Proc. Roy. Soc. London A* **324**, 301-313.

Johansen, A., A. C. Andersen, and A. Brandenburg 2004 Simulations of dust-trapping vortices in protoplanetary discs *Astron. Astrophys.* **417**, 361-374.

Kusaka, T., T. Nakano and C. Hayashi 1970. Growth of Solid Particles in the Primordial Solar Nebula *Prog. Theor. Phys.* **44**, 1580-1595.

Mizuno, H., W. J. Markiewicz. and H. J. Voĭk 1988. Grain growth in turbulent protoplanetary accretion disks *Astron. Astrophys.* **195**, 183-192.

Mizuno, H. 1989. Grain growth in the turbulent accretion disk solar nebula. *Icarus* **80**, 189-201.

Nakagawa, Y., K. Nakazawa, and C. Hayashi 1981. Growth and sedimentation of dust grains in the primordial solar nebula. *Icarus* **45**, 517-528.

Nakagawa, Y., M. Sekiya, and C. Hayashi 1986. Settling and growth of dust particles in a laminar phase of a low-mass solar nebula. Icarus **67**, 375-390.

Ohtsuki, K., Y. Nakagawa, and K. Nakazawa, 1990. Artificial acceleration in accumulation due to coarse mass-coordinate divisions in numerical simulation *Icarus* **83**, 205-215.

Pollack, J. B., D. Hollenbach, S. Beckwith, D. P. Simonelli, T. Roush, and W. Fong 1994. Composition and radiative properties of grains in molecular clouds and accretion disks *Astrophys. J.* **421**, 615-639.

Safronov V. S 1969 Evolution of the Protoplanetary Cloud and Formation of the Earth and the Planets (NASA Tech. Trans. F-677) (Nauka: Moscow).

Schmitt, W., T. Henning, and R. Mucha 1997. Dust evolution in protoplanetary accretion disks *Astron. Astrophys.* **325**, 569-584

Shakura, N. I., and R. A. Sunyaev 1973. Black holes in binary systems. comets. In From Plasma to Planet, Proceedings of the Nobel Symposium Observational appearance. *Astron. Astrophys.* **24**, 337-355.

Schräpler, R., and T. Henning 2004. Dust diffusion, sedimentation, and gravitational instabilities in protoplanetaty disks. *Astrophys. J.* **614**, 960-978.

Sirono, S., and J. M. Greenberg 2000. Do cometesimal collisions lead to bound rubble piless or to aggregates held together by gravity? *Icarus* **145**, 230-238.

Tanga, P., A. Babiano, B. Dubrulle, and A. Provenzale 1996. Forming planetesimals in vortices. *Icarus* **121**, 158.

Tanaka., H and Y. Himeno and S. Ida 2005. Dust growth and settling in protoplanetary disks and disk spectral energy distributions. I. laminar disks. *Astrophys. J.* **625**, 414-426

Tennekes, H., and J. L. Lumley 1972. A First Course in Turbulence. MIT Press, Cambridge, MA.

Takeuchi, T., and D. N. C. Lin 2002. Radial flow of dust particles in accretion disks.*Astrophys. J.*, **581**, 1344-1355

Testi, L., A. Natta, D. S. Shepherd, and D. J. Wilner 2003. Large grains in the disk CQ Tau *Astron. Astrophys.* **403**, 323-328

van Boekel, R., L. B. F. M. Waters, C. Dominik 2003. Grain growth in the inner regions of Herbig Ae/Be star disks? *Astron. Astrophys.* **400**, L21-L24.

Völk, H. J., F. C. Jones, G. E. Morfill, and S. Ro̧ser 1980. Collisions between grains in a turbulent gas. *Astron. Astrophys.* **85**, 316-325.

van Leer, B. 1977. Towards the Ultimate Conservation Difference Scheme. 4, A New Approach to Numerical Convection. *J. Comput. Phys.*, **23**, 276-299

Meakin, P., and B. Donn, 1988, Aerodynamic properties of fractal grains:implications for the primordial solar nebula *Astrophys J.* **329**, L39-L41.

Weidenschilling, S. J., and J. N. Cuzzi 1993. Formation of planetesimals in the solar nebula. In Protostars and Planets III (E. H. Levy and J. I. Lunine, Eds.), pp. 1031?1060. Univ. of Arizona Press, Tucson.

Weidenschilling, S. J. 1980. Dust to planetesimals - Settling and coagulation in the solar nebula *Icarus* **44**, 172-189

Weidenschilling, S. J. 1984. Evolution of grains in a turbulent solar nebula *Icarus* **60**, 553-567.

Weidenschilling, S. J. 1997. The origin ofcomets in the solar nebula: a unified Model *Icarus* **127**, 290-306.

Whipple, F. L. 1972. in From Plasma to Planet, ed. A. Elvius (London:Wiley), 211

Wurm, G., and J. Blum 1998. Experiments on preplanetary dust aggregation. *Icarus* **132**, 125-136.